

# Reorganization of the Flagellum Scaffolding Induces a Sperm Standstill During Fertilization


Reviewed Preprint

v2 • September 3, 2024

Revised by authors

Reviewed Preprint

v1 • January 18, 2024

**Martina Jabłoński, Guillermina M Luque, Matías D Gómez-Elías, Claudia Sanchez-Cardenas, Xinran Xu, Jose Luis de la Vega-Beltran, Gabriel Corkidi, Alejandro Linares, Víctor X Abonza Amaro, Aquetzalli Arenas-Hernandez, María Del Pilar Ramos-Godinez, Alejandro López-Saavedra, Dario Krapf, Diego Krapf, Alberto Darszon, Adan Guerrero, Mariano G Buffone** 

Instituto de Biología y Medicina Experimental, Consejo Nacional de Investigaciones Científicas y Técnicas (IBYME-CONICET), Buenos Aires, Argentina • Departamento de Genética del Desarrollo y Fisiología Molecular, Instituto de Biotecnología, Universidad Nacional Autónoma de México, Cuernavaca, Mexico • Department of Electrical and Computer Engineering and School of Biomedical Engineering, Colorado State University, Fort Collins, USA • Laboratorio de Imágenes y Visión por Computadora, Instituto de Biotecnología, Universidad Nacional Autónoma de México, Cuernavaca, México • Laboratorio Nacional de Microscopía Avanzada, Instituto de Biotecnología, Universidad Nacional Autónoma de México, Cuernavaca, Mexico • Departamento de Microscopía Electrónica, Instituto Nacional de Cancerología, Mexico City, Mexico • Unidad de Aplicaciones Avanzadas en Microscopía, Instituto Nacional de Cancerología, Unidad de Investigación Biomédica en Cáncer, UNAM. Mexico City, Mexico • Tecnológico de Monterrey, Escuela de Medicina y Ciencias de la Salud. Mexico City, Mexico • Instituto de Biología Molecular y Celular de Rosario (IBR), Consejo Nacional de Investigaciones Científicas y Técnicas (CONICET), Universidad Nacional de Rosario (UNR), Rosario, Argentina

 [https://en.wikipedia.org/wiki/Open\\_access](https://en.wikipedia.org/wiki/Open_access)

 Copyright information

## Abstract

Mammalian sperm delve into the female reproductive tract to fertilize the female gamete. The available information about how sperm regulate their motility during the final journey to the fertilization site is extremely limited. In this work, we investigated the structural and functional changes in the sperm flagellum after AE and during the interaction with the eggs. The evidence demonstrates that the double helix actin network surrounding the mitochondrial sheath of the midpiece undergoes structural changes prior to the motility cessation. This structural modification is accompanied by a decrease in diameter of the midpiece and is driven by intracellular calcium changes that occur concomitant with a reorganization of the actin helicoidal cortex. Midpiece contraction occurs in a subset of cells that undergo AE, live-cell imaging during in vitro fertilization showed that the midpiece contraction is required for motility cessation after fusion is initiated. These findings provide the first evidence of the F-actin network's role in regulating sperm motility, adapting its function to meet specific cellular requirements during fertilization, and highlighting the broader significance of understanding sperm motility.

## Significant statement

In this work, we demonstrate that the helical structure of polymerized actin in the flagellum undergoes a rearrangement at the time of sperm-egg fusion. This process is driven by

intracellular calcium and promotes a decrease in the sperm midpiece diameter as well as the arrest in motility, which is observed after the fusion process is initiated.

### eLife assessment

This **important** work substantially advances our understanding of sperm motility regulation during fertilization process by uncovering the midpiece/mitochondria contraction associated with motility cessation and structural changes in the midpiece actin network as its mode of action involved. The evidence supporting the conclusion is **solid**, with rigorous live cell imaging using state-of-art microscopy, although more functional analysis of the midpiece/mitochondria contraction would have further strengthened the study. The work will be of broad interest to cell biologists working on the cytoskeleton, mitochondria, cell fusion, and fertilization.

<https://doi.org/10.7554/eLife.93792.2.sa3>

## Introduction

Sperm motility is required for arrival at the site of fertilization and to penetrate the different layers surrounding the egg. The temporal regulation of sperm motility involves the concerted action of multiple cell structures to enable fertilization. The initial motility of ejaculated sperm is characterized by a linear progressive movement as the cells traverse a long distance within the female reproductive tract. However, at one point, before reaching the oocyte, this initial progressive motion must be changed to a vigorous non-progressive mode of motility called hyperactivation (1). During that migration, most of mouse sperm undergo acrosomal exocytosis (AE), which takes place in the upper segments of the oviduct, before the sperm directly interact with the egg or its surrounding layers (2–4). This exocytic event is critical because proteins involved in this process are rearranged in preparation for fusion (5, 6). A second dramatic change in motility is subsequently required for efficient sperm-egg fusion. During this event, which has not been studied in detail so far, sperm completely stop moving (7–9). The cease in sperm motility is considered as an indicative marker of an effective fusion between gametes, given that it is necessary to complete the attachment and fusion between sperm and eggs. Fusion itself is a complex event mediated by several proteins identified using loss of function strategies (10, 11). Nevertheless, the available information about how sperm regulate their motility during the final journey to the fertilization site and during the interaction with the female gamete is extremely limited. In this final journey, most sperm cells migrate to the ovulated eggs after AE, and very little is known about the motility state of those sperm and about the molecular mechanism in charge of the motility arrest.

The regulation of sperm motility is achieved by balancing force transduction and the mechanical properties of the flagellum. Both effects are governed by the flagellum cytoskeleton, which consists of two major components: a microtubule-based axoneme, located at the flagellum axis, and actin filaments around it (12). The midpiece and the principal piece also contain the outer dense fibers and the fibrous sheath that have traditionally been referred to as part of the sperm cytoskeleton. Recently it was found that the three-dimensional organization of polymerized actin in the flagellum midpiece of murine sperm forms a unique double helix arrangement accompanying mitochondria (13). This spatial distribution does not extend into the principal piece, where actin is uniformly distributed between the axoneme and the plasma membrane. Across all investigated cells, this double helix consisted of exactly 87 gyres with a pitch of  $244 \pm 1$  nm, yielding a total midpiece length in mice of  $21.2 \pm 0.3$   $\mu$ m (13). Such accurate control of sizes is

not typical in live cells given that reactions are prone to stochastic effects and entropy leads to large cell-to-cell fluctuations. Thus, the precise control of the actin helix comes at a substantial regulatory cost for sperm cells. Nevertheless, the function of this specialized structure of actin filaments is largely unknown.

In this work, we find definite evidence for the role of the helical actin structure in the final stage of motility regulation, when sperm dramatically shift from being hyperactivated to a practically immotile stage. We have investigated the structural changes in the actin cytoskeleton of the sperm flagellum after AE and during the interaction with the eggs. By using a combination of single-cell imaging and super-resolution microscopy methods, our results demonstrate that the helical structure of polymerized actin undergoes a radical structural change at the time of sperm-egg fusion. Further, we uncover that this process is triggered by a substantial calcium ( $[Ca^{2+}]_i$ ) influx. This actin-dependent signaling pathway promotes a decrease of the sperm midpiece diameter and motility arrest, both of which are found to be required to complete the fusion process during fertilization.

## Results

### AE promotes a cessation of motility in a subset of sperm cells

After AE, sperm need to accomplish migration to the ampulla, reach unfertilized eggs, penetrate the cumulus matrix and the zona pellucida and finally, undergo fusion with the oocyte (14 [↗](#)). All these processes share the need to modulate sperm motility. Little is known about the regulation of motility after the occurrence of AE or prior to the fusion with the oocyte.

To simultaneously monitor the acrosomal status and sperm motility in live cells, transgenic mice whose sperm express enhanced green fluorescent protein (EGFP) in the acrosome and red fluorescent protein (DsRed2) in the mitochondria were used (Figure 1A [↗](#), Supplementary movie S1). EGFP-DsRed2 sperm were immobilized at the head on laminin-coated coverslips, while still allowing free flagellar movement (Figure 1B [↗](#), Supplementary movie S2). While the presence of the acrosome is monitored using the EGFP fluorescence signal, motility was assessed through the movement of the midpiece (DsRed2 fluorescence), which was beating in and out of the imaging plane (Figure 1B [↗](#)).

The majority of acrosome-intact sperm were able to move. Interestingly, Figures 1B [↗](#) and 1C [↗](#) show the coexistence of two populations of sperm that underwent AE (cells lacking EGFP signal) induced upon addition of progesterone, a physiological trigger of AE. Some of the acrosome reacted sperm moved normally ( $34.1 \pm 3.7\%$ ,  $n = 235$ ), whereas the majority of them remained immotile ( $65.9 \pm 6.2\%$ ,  $n = 2350$ ) (Figures 1B [↗](#) and 1C [↗](#), upper and lower panel, respectively, Supplementary movie S2).

The flagellar beat cycle encompasses a self-regulatory mechanism that receives feedback from molecular and mechanical signals (15 [↗](#)). The complete abortion of flagellar beat cycle observed in Figures 1B [↗](#) and 1C [↗](#) might be indicative of a stimulus provided by or occurring concomitant with AE. To comprehend the connection between AE and motility, we hypothesized the existence of a mechanical change in the flagella as a result of the AE. For this reason, AE was studied in the presence of FM4-64 fluorescent dye (16 [↗](#)) to visualize structural changes at the plasma membrane, which can occur at macroscopic scales observed as an alteration in the shape of the flagellum, or at mesoscopic scales, monitored by local changes in FM4-64 fluorescence occurring at the vicinity or within the plasma membrane. EGFP-DsRed2 sperm were stimulated with progesterone and their 'motility' behavior was recorded for 5 min in the presence of FM4-64. The loss of EGFP fluorescence in the acrosome of transgenic mice correlated with a noticeable increase of FM4-64 fluorescence in the head, as shown in Figure 1D [↗](#) (see panels 0' and 3', Supplementary

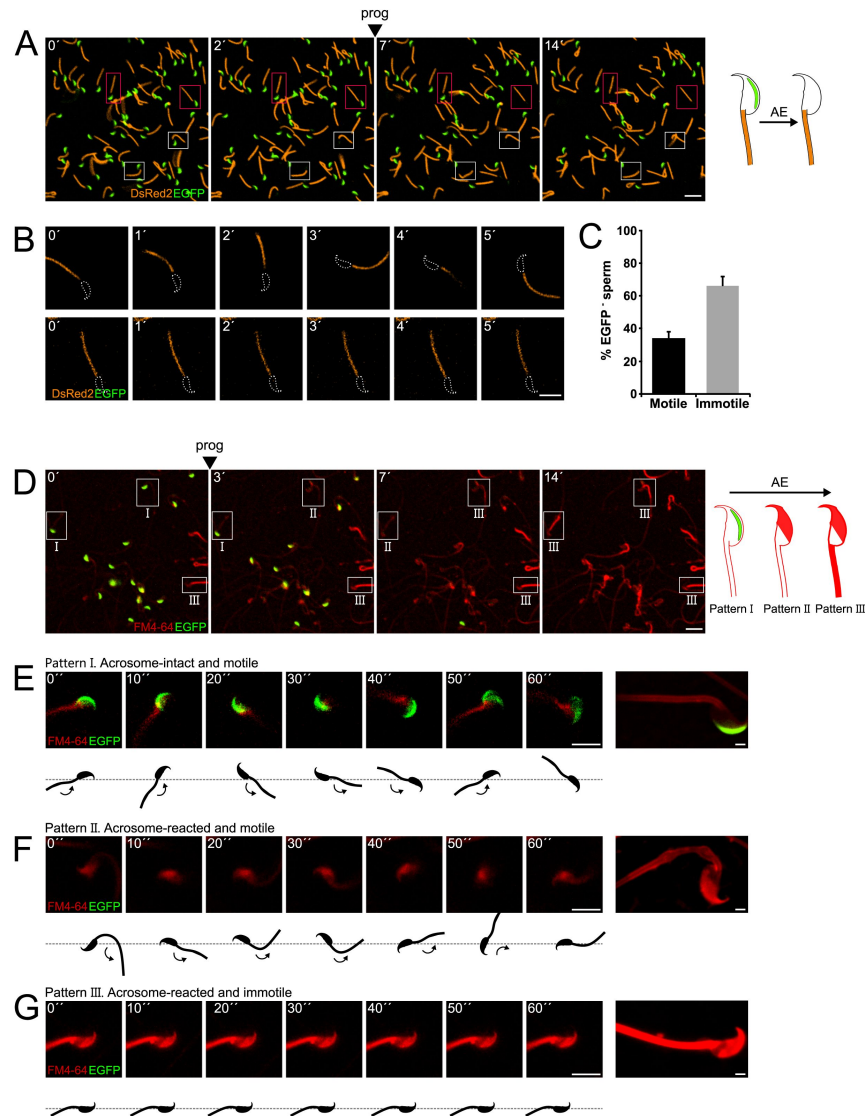


**Figure 1.**

### Sperm motility loss and FM4-64 fluorescence dynamics in acrosome-reacted transgenic EGFP-DsRed2 sperm.

A) Representative time series of transgenic EGFP-DsRed2 sperm attached to concanavalin A-coated coverslips, with AE induced by 100  $\mu$ M progesterone. White squares indicate cells with spontaneous AE (prior to induction), while pink squares highlight cells with progesterone-induced AE. A schematic representation of AE in this transgenic model is shown on the right side of the panel. Scale bar = 20  $\mu$ m. B) Representative time series of transgenic EGFP-DsRed2 sperm that have already experienced AE, attached to laminin-coated coverslips. The upper panel displays a cell with motility after AE, and the lower panel shows an immotile cell. DsRed2 is presented in orange, and EGFP in green. Scale bar = 10  $\mu$ m. C) Quantification of motile and immotile acrosome-reacted sperm (EGFP<sup>+</sup>). A total of 235 cells were counted across at least three independent experiments. D) Representative time series of transgenic EGFP-DsRed2 sperm stained with 10  $\mu$ M FM4-64 and attached to concanavalin A-coated coverslips, with AE induced by 100  $\mu$ M progesterone. White squares indicate cells exhibiting patterns I, II, or III after progesterone induction. Scale bar = 20  $\mu$ m. A schematic representation of AE in this transgenic model stained with FM4-64 is shown on the right side of the panel. E-G) Representative images of capacitated transgenic EGFP-DsRed2 sperm stained with 10  $\mu$ M FM4-64. Panel E) displays an acrosome-intact, motile sperm (Pattern I), F) shows an acrosome-reacted sperm with motility and low FM4-64 midpiece fluorescence (Pattern II), and G) presents an acrosome-reacted sperm with no motility and high FM4-64 midpiece fluorescence (Pattern III). In all three cases, cells were induced with 100  $\mu$ M progesterone. Scale bar = 10  $\mu$ m. Enlarged images of each pattern are shown on the right panel. Scale bar = 2  $\mu$ m. Representative images from at least five independent experiments are displayed.

movie S3). In addition, we noticed that sperm that underwent AE, later showed an increase in the FM4-64 fluorescence intensity in the flagellum as well (see panel 14' of **Figure 1D** [↗](#), Supplementary movie S3).

A more detailed analysis of individual cells demonstrated changes in FM4-64 fluorescence according to their motility (Supplementary movie S4). **Figure 1E** [↗](#) shows a motile acrosome-intact sperm, (a control case), where the fluorescence levels of EGFP and FM4-64 remained constant during the entire experiment (Pattern I). Interestingly, sperm that lost their acrosome (no EGFP and high FM4-64 fluorescence in the sperm head) and continued moving, presented low levels of FM4-64 fluorescence in the midpiece (**Figure 1F** [↗](#), Pattern II). On the other hand, acrosome-reacted sperm that remained immotile showed a significant rise in the FM4-64 midpiece fluorescence (**Figure 1G** [↗](#), Pattern III). Noteworthy, both subsets of cells (with and without motility) displayed the expected increase in FM4-64 fluorescence in the sperm head.

To deepen our understanding on how sperm lose motility during AE, we designed a sperm tracking system that can also monitor changes in fluorescence in moving cells (Figure S1B and S1C). Three parameters were then assessed in real time, namely, the beat frequency of the flagellum (by tracking it on bright field images, or the DsRed2 channel, Figure S1A), the status of the acrosome (EGFP signal), and changes occurring at or within the membrane in the midpiece (FM4-64 signal). Figure S1B shows that sperm that did not undergo AE remained motile with a stable beat frequency and low FM4-64 fluorescence over the recording time. In stark contrast, after AE, cells gradually diminished the beating frequency until a complete arrest is observed, while a gradual increase in FM4-64 fluorescence in the midpiece is observed (Figure S1C).

To evaluate the relationship between FM4-64 and viability, a vital dye Sytox Blue was used in imaging flow cytometry experiments. Fluorescence intensities in non-capacitated sperm stimulated with ionomycin (Figure S1D) were determined and two populations with Sytox Blue signals were clearly distinguished (Sytox+ and Sytox-), enabling the discernment between live and dead sperm. Interestingly, the upper right panels (Sytox Blue+ / FM4-64 high) consistently show a positive correlation between FM4-64 and Sytox Blue. Nonetheless, the lower panels (Sytox Blue-) show no correlation with FM4-64 fluorescence, indicating that this population can exhibit either low or high FM4-64 fluorescence. Single-cell examples are shown, where the four categories are represented: dead sperm with low FM4-64 fluorescence (Sytox Blue + / FM4-64 low), dead sperm with high FM4-64 fluorescence (Sytox Blue + / FM4-64 high), live sperm with low FM4-64 fluorescence (Sytox Blue - / FM4-64 low), and live sperm with high FM4-64 fluorescence (Sytox Blue - / FM4-64 high). Therefore, while the FM4-64 signal alone is not a definitive marker for either AE or cell death, it is crucial to use additional viability assessments, such as Sytox Blue, to accurately differentiate between live and dead sperm in studies of acrosome exocytosis and sperm motility. Cell viability was always considered, as any imaged sperm was chosen based on motility, indicated by a beating flagellum. The determination of whether selected sperm die during or after AE remains to be elucidated. The results presented in **Figure 1** [↗](#) and Supplementary Figure S1 show examples of motile sperm that experience an increase in FM4-64 fluorescence.

Altogether, these experiments demonstrate that AE promotes a cease of motility in a subset of sperm cells, which coincides with an increase in FM4-64 fluorescence in the midpiece.

## AE is followed by a decrease in the midpiece diameter

Live-cell super-resolution microscopy was used to understand the structural changes occurring in the midpiece. **Figure 2A** [↗](#) shows a wide-field image of a sperm midpiece stained with FM4-64 (left) and analyzed using super-resolution radial fluctuations (SRRF, right) ([17](#) [↗](#)). AE dynamics was monitored by FM4-64 fluorescence in the head (**Figure 2B** [↗](#), upper right insets). A decrease in the midpiece diameter over time was observed following AE either being spontaneous, induced by a physiological agonist (progesterone), or induced by a non-physiological surge of  $\text{Ca}^{2+}$  (ionomycin) (**Figures 2B** [↗](#) and **2C** [↗](#) and Supplementary movie S5). In the negative control (no

AE), the diameter remained unchanged. This phenomenon was also observed using mean shift super-resolution (MSSR) (18). To further support this observation, other plasma membrane probes of different molecular structure, such as Memglow 700 (Figure S2A), Bodipy-GM1 (Figure S2B), and FM1-43 (Figure S2C), were used. In all three cases, a decrease in the midpiece diameter was observed after AE.

The FM4-64 fluorescence intensity in the head and in the midpiece (Figures 2D and 2E) were also assessed. As expected, the increase in FM4-64 fluorescence in the head occurs after AE. Furthermore, in agreement to what was observed in Figure 1, fluorescence intensity in the midpiece also increased over time in sperm that underwent AE (Figures 2D and 2E).

To confirm these results, two alternative methods to visualize the change in sperm midpiece diameter were used. In neither of them, a membrane dye was used. First, indirect immunofluorescence to detect a membrane protein (GLUT3) was performed. As shown in Figure 2G, a decrease in the midpiece diameter was also observed. Second, scanning electron microscopy (SEM) was used to evaluate the midpiece in acrosome-intact or reacted sperm (Figure 2F). The overall diameter of the midpiece in acrosome-intact sperm was larger than in acrosome-reacted sperm, with measurements of  $0.731 \pm 0.008 \mu\text{m}$  and  $0.694 \pm 0.007 \mu\text{m}$ , respectively. Overall, we have confirmed using three different approaches that AE is followed by a midpiece diameter.

## The contraction of the midpiece initiates in the proximal part of the flagellum

To investigate whether the contraction of the midpiece is triggered at a random location or in a particular region of the flagellum, kymographs were used. A kymograph allows visualization of dynamical aspects of a given phenomenon in a single figure, where the temporal dimension is expressed as an axis of the image through a spatial-temporal transformation of the dataset. Two types of kymographs were used (Figure 3A). First, super-resolution microscopy kymographs were built to monitor dynamic changes in the diameter of the flagellum along the midpiece. Second, to investigate the number of contraction sites, fluorescence kymographs were made from diffraction-limited images to observe changes in FM4-64 fluorescence over time and across the entire midpiece. Interestingly, Figure S2D shows a significant negative correlation between the midpiece diameter and the FM4-64 fluorescence, unveiling a tool to obtain an approximate value of the midpiece diameter without the need of super-resolution microscopy.

Three experimental subsets that underwent AE were assessed: spontaneous, induced by progesterone, and induced by ionomycin. To scrutinize randomness of focus-driven contraction, the midpiece was segmented in three regions (Figure 3A): proximal (near the neck), central, and distal (near the annulus). In these groups, it was then evaluated whether cells presented one or more foci of contraction.

Figure 3B shows a cumulative study, which indicates that contraction is preferentially initiated at the proximal part of the midpiece, regardless of being progesterone-induced or spontaneous AE. When ionomycin was used as an agonist of AE, the contraction began randomly in any segment of the midpiece. Figures 3C and 3D show two examples of flagellar dynamics for progesterone-induced sperm, which either presented one or two foci of contraction. In both cases, the diameter decreased along the whole midpiece, seen as a transition from dark to bright red colors in Figures 3C and 3D. Noteworthy, focal points of contraction were consistently observed: i.e., a case with a single focus (Figure 3C), or a case with two foci of contraction (Figure 3D). Figures S2E and S2F show ionomycin-induced sperm that present one or more foci. It is observed in the normalized diameter kymograph that the flagellum presents a single focus between the measurements of  $7.5 \mu\text{m}$  and  $10 \mu\text{m}$  (Figure S2E, left panel). This is reflected in the right panel in the light blue and orange dots, which are the actual diameter measurements that decreased first



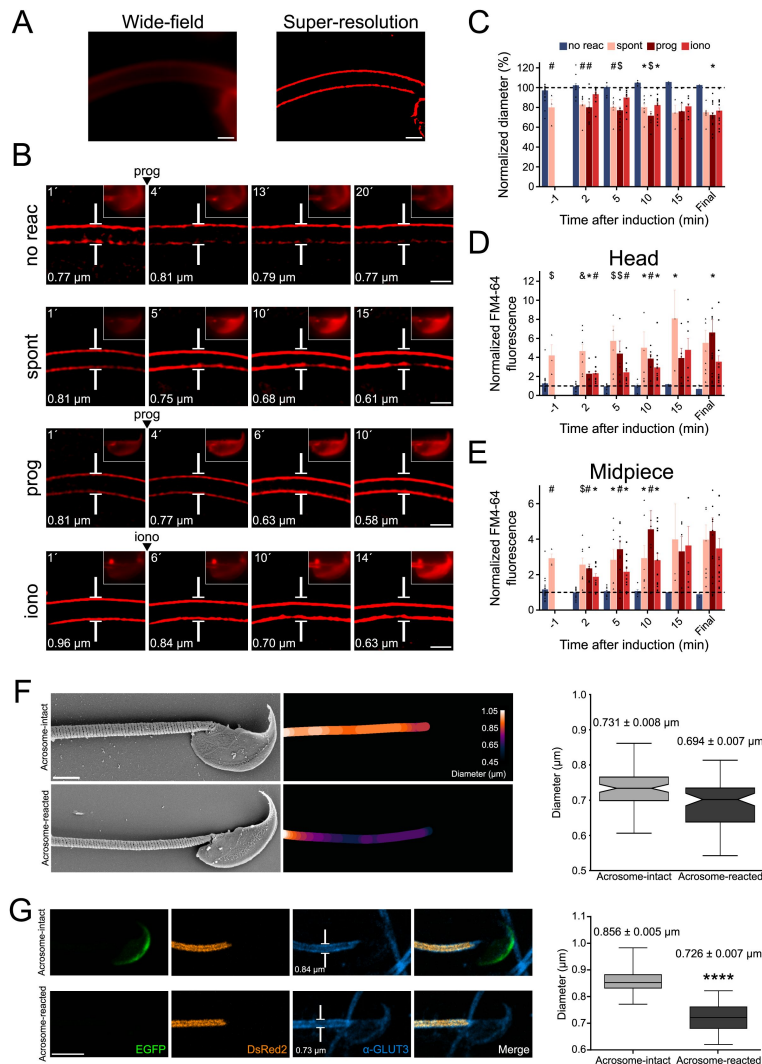


**Figure 2.**

### Midpiece contraction coincides with the onset of AE.

A) Left panel displays a wide-field fluorescence image of capacitated CD1 sperm membrane stained with 0.5  $\mu$ M FM4-64, while the right panel shows its super-resolution SRRF reconstruction. Scale bar = 1  $\mu$ m. B) Representative time series of sperm midpiece with no AE (no reac), spontaneous exocytosis (spont), progesterone (prog, 100  $\mu$ M) and ionomycin-induced (iono, 10  $\mu$ M) exocytosis, respectively. Following acquisition, images were analyzed using SRRF. Insets in the sperm head show wide-field images of AE. The midpiece diameter value is displayed in the bottom left corner for each time point. Scale bar = 1  $\mu$ m. C) Quantification of midpiece diameter changes for each experimental group across time. Data are presented as a percentage of the initial diameter value before induction for each cell. D-E) Quantification of FM4-64 fluorescence in the sperm head and midpiece, respectively, for each experimental group across time. Data are presented as times of increases compared to initial fluorescence before AE induction. \* $p$ <0.05; # $p$ <0.01; \$ $p$ <0.001 and & $p$ <0.0001 compared to the non-reacted group. A nonparametric Kruskal-Wallis test was performed in combination with Dunn's multiple comparisons test. Representative images of at least 5 independent experiments are shown, with 36 cells analyzed. F) Comparison of the midpiece architecture in acrosome-intact (AI, upper panel) and acrosome-reacted (AR, lower panel) sperm using scanning electron microscopy (SEM). Representative images are shown, middle panels show quantification of these images whereas the left panel shows the quantification of all replicates. Data is presented as mean  $\pm$  SEM, Kruskal-Wallis test was employed,  $p$  = 0.013, (AI  $n$ =85, AR  $n$ =72). Scale bar = 2  $\mu$ m. G) Capacitated transgenic EGFP-DsRed2 sperm were induced by 100  $\mu$ M progesterone. Cells were fixed and immunostained against -GLUT3 in order to see the plasma membrane in the midpiece. Representative images of at least 2 independent experiments are shown. Left panel shows quantification of midpiece diameter in acrosome-intact and acrosome-reacted EGFP-DsRed2 sperm. Data is presented as mean  $\pm$  sem. A nonparametric Mann Whitney test was performed, \*\*\*\* $p$ <0.001 (AI  $n$ =84, AR  $n$ =47). Scale bar = 5  $\mu$ m.

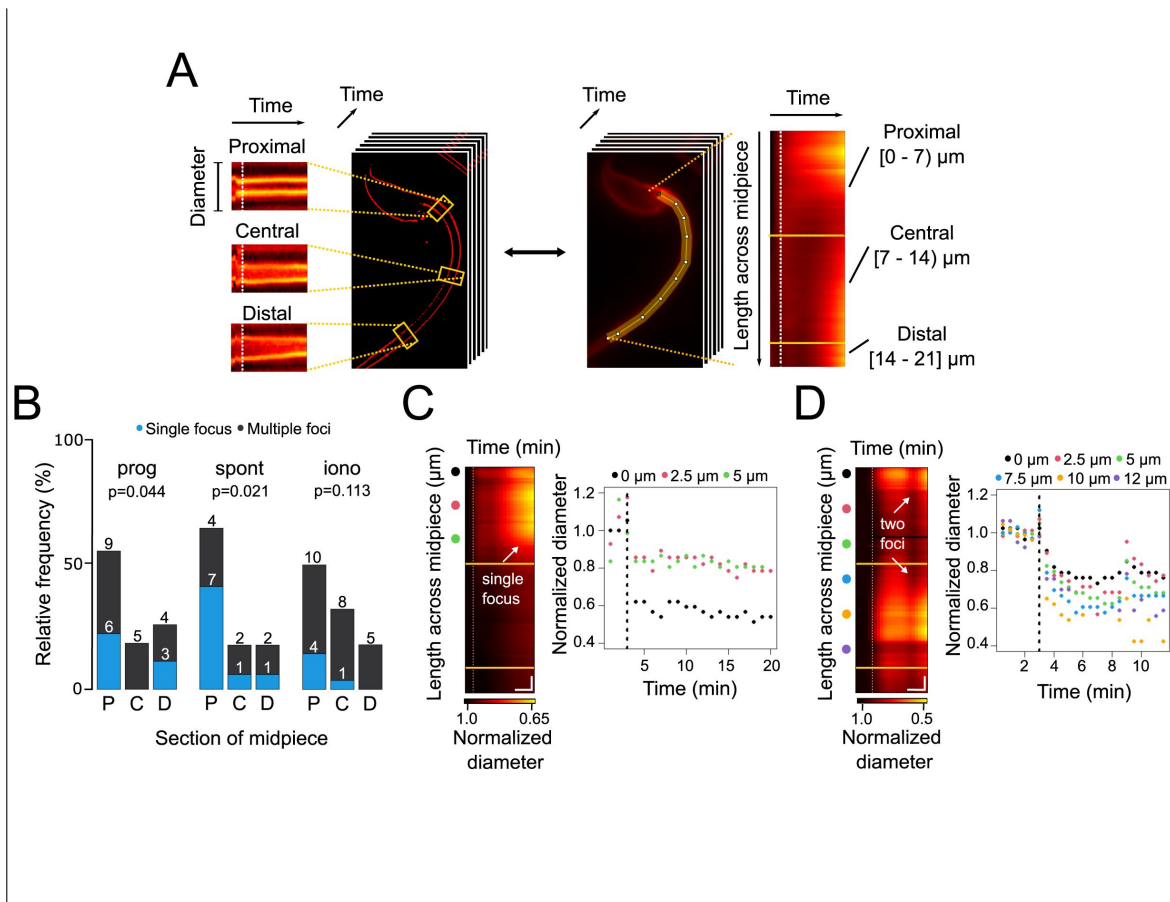


**Figure 3.**

### Contraction initiation preferentially occurs near the head-midpiece junction.

A) Schematic diagram illustrating the generation of super-resolution kymographs from SRRF-processed images. Crosslines are drawn every 2.5  $\mu\text{m}$  through the sperm midpiece, and the Image-J Kymograph builder plug-in is used to create kymographs. The x-axis represents time, and the y-axis shows diameter changes. For wide-field images, a line along the midpiece is drawn to create fluorescence kymographs, with the y-axis representing midpiece length. Three sections of the midpiece are defined: proximal [0-7  $\mu\text{m}$ ], central [7-14  $\mu\text{m}$ ], and distal [14-21  $\mu\text{m}$ ]. B) Relative frequency graph displaying the distribution of the initiation sites for midpiece contractions in sperm with no AE (no reac), spontaneous exocytosis (spont), progesterone-induced (prog, 100  $\mu\text{M}$ ) exocytosis, and ionomycin-induced (iono, 10  $\mu\text{M}$ ) exocytosis, respectively. The x-axis indicates the midpiece section where the contraction begins: proximal (P), central (C), or distal (D). A  $\chi^2$  test was performed using the R language environment. C-D) Representative contraction kymographs and diameter measurements for progesterone-induced (100  $\mu\text{M}$ ) AE with one or two contraction initiation sites, respectively. In contraction kymographs, yellow lines demarcate midpiece sections, and colored spots indicate where super-resolution kymographs were created. Both kymograph and diameter measurement graphs display a dotted vertical line marking the induction point. For C, horizontal scale bar = 5 min and vertical scale bar = 1  $\mu\text{m}$  and for D, horizontal scale bar = 3 min and vertical scale bar = 1  $\mu\text{m}$ . Data from at least 5 independent experiments are shown, with 36 cells analyzed.



and most (Figure S2E). A representative behavior within this experimental group is represented in Figure S2F, where the entire midpiece contracted (all its sections simultaneously). This is observed in the color scale of the normalized diameter kymograph and coincides with the real measurements of the diameter in the right panel, which decreased their value. Lastly, Figures S2G and S2H show examples of spontaneous AE with one or two foci of contraction, respectively. In particular, in Figure S2H, a first focus of contraction between 0 and 5  $\mu\text{m}$  that coincided with the diameter measurements of the right panel that decreased their value first and to a greater extent (black, pink and green dots). Although the entire midpiece contracted, a second focus of contraction appeared around the measurements of 10 to 15  $\mu\text{m}$  and coincidentally, these are the points with the strongest decrease in the diameter (orange, purple and red points).

## The reduction of the midpiece diameter occurs concomitantly with a $[\text{Ca}^{2+}]_i$ increase in the flagellum

It is widely accepted that an increase in  $[\text{Ca}^{2+}]_i$  precedes AE (16, 19). It has been shown that AE initiation by progesterone occurs after an increase in  $[\text{Ca}^{2+}]_i$  in the sperm head that is later propagated towards the midpiece (19). To comprehend the connection between AE and the concomitant contraction of the midpiece, we hypothesized the existence of a signal, i.e.,  $\text{Ca}^{2+}$ , which propagates from the head to the flagellum and modulate the architecture of the sperm flagellum.

To investigate if the increase in the concentration of  $[\text{Ca}^{2+}]_i$  in the midpiece is correlated with the midpiece contraction, sperm were incubated with FM4-64 and Fluo4, a  $\text{Ca}^{2+}$  fluorescent sensor (Supplementary movie S6). **Figure 4A** shows a live-cell imaging experiment of sperm cells that did not undergo AE (control case), nor a significant rise in  $[\text{Ca}^{2+}]_i$ . Noteworthy, upon induction with progesterone (**Figure 4C**, Supplementary movie S6), there was an increase in the midpiece  $[\text{Ca}^{2+}]_i$  followed by an increase in FM4-64 fluorescence, which is indicative of a contraction of the flagellum (see Figure S2D). These single cell experiments illustrate a reduction of the midpiece diameter that occurs concomitantly with an increase in  $[\text{Ca}^{2+}]_i$  within the flagellum. A large population of sperm was analyzed using low magnification (10X). **Figures 4B** and **4D** show a collection of single cell kymographs, where each row represents the fluorescence of Fluo4 (green) and FM4-64 (red) of the midpiece over time. Unstimulated cells are displayed on **Figure 4B** and sperm that were exposed to progesterone are shown in **Figure 4D**. Most of the cells display a transient  $[\text{Ca}^{2+}]_i$  increase followed by an increase in FM4-64 fluorescence. This pattern was also observed in ionomycin-induced cells (Figures S3A and S3B and Supplementary movie S6) with the exception that, as expected, in this case the rise in  $[\text{Ca}^{2+}]_i$  was faster and sustained. These findings indicate that an  $[\text{Ca}^{2+}]_i$  transient increase, happening in the midpiece, precedes the contraction of the flagellum.

The relationship between the observed  $[\text{Ca}^{2+}]_i$  rise and the flagellar contraction was then assessed using live-cell super-resolution imaging. **Figure 4E** shows there is a  $[\text{Ca}^{2+}]_i$  increase in the midpiece that coincides in space and time with a contraction of the midpiece. To provide insight in the spatio-temporal relationship of the  $[\text{Ca}^{2+}]_i$  rise and the midpiece contraction, these results were visualized using a 3D kymograph encompassing the dynamics happening along the entire midpiece (**Figure 4F**). Overall, a rise in  $[\text{Ca}^{2+}]_i$  occurred along the whole midpiece, which coincided with a generalized contraction of the midpiece (**Figure 4F**). Remarkably, a transient focal increase of  $[\text{Ca}^{2+}]_i$  was observed at the base of the flagellum, which correlates in space and time with a focal reduction of the diameter (**Figure 4F**). We then sought to identify a molecular/structural link between both processes.

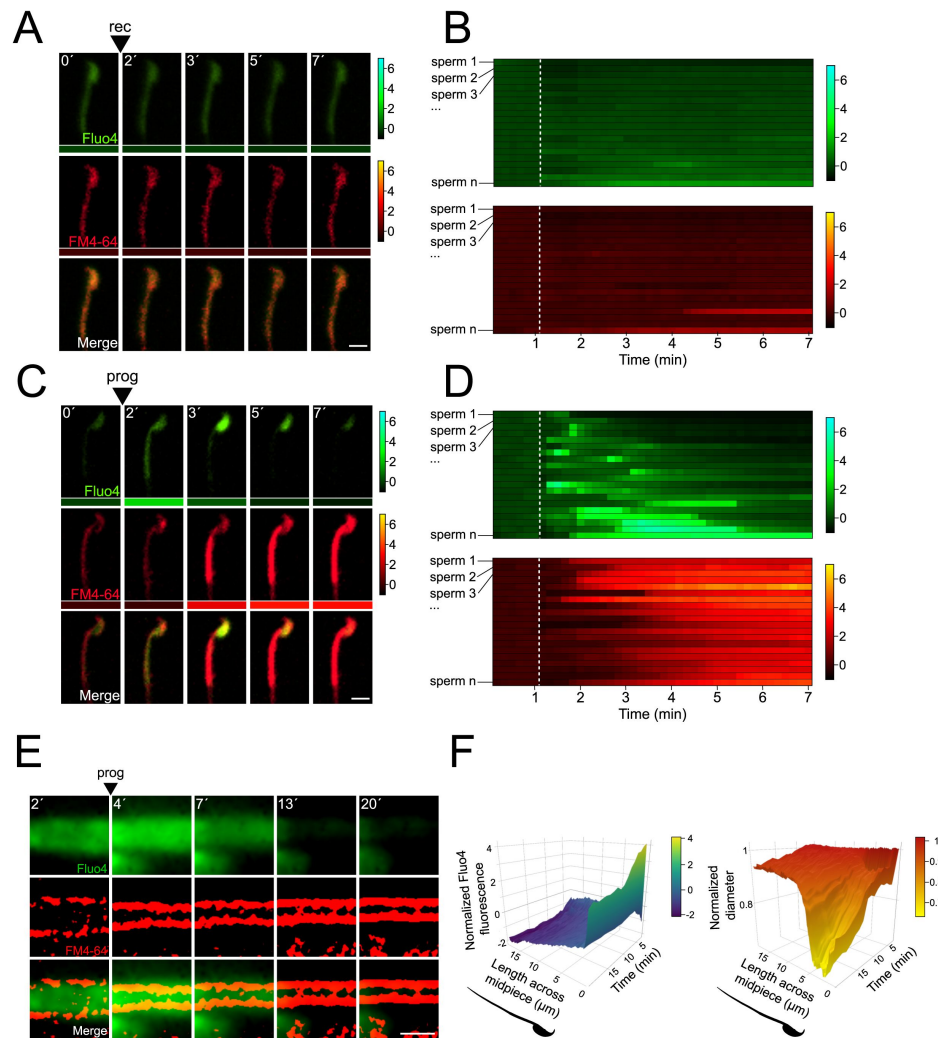


**Figure 4.**

### Midpiece contraction is driven by $[Ca^{2+}]_i$ changes.

A) The representative time series demonstrates  $[Ca^{2+}]_i$  and AE dynamics. Capacitated F1 sperm, loaded with Fluo4 AM, were immobilized on concanavalin A-coated coverslips and incubated in a recording medium (rec) containing 10  $\mu$ M FM4-64. Rec was added as indicated by arrowheads. Scale bar = 10  $\mu$ m. Beneath each frame in the Fluo4 (green) and FM4-64 (red) images, a color code displays the normalized intensity of the fluorescence signal (scale bar on the right of the panel). B) Kymograph-like analysis of the midpiece of 20 sperm following the addition of recording medium. Each row depicting the  $[Ca^{2+}]_i$  (upper) and membrane (lower) dynamics of a single cell over time. A white dotted line indicates the moment of addition. The images presented are representative of at least five independent experiments. C) The representative time series demonstrates  $[Ca^{2+}]_i$  and AE dynamics. Progesterone (prog, 100  $\mu$ M) was added as indicated by arrowheads. Scale bar = 10  $\mu$ m. Beneath each frame in the Fluo4 (green) and FM4-64 (red) images, a color code displays the normalized intensity of the fluorescence signal (scale bar on the right of the panel). D) Kymograph-like analysis of the midpiece of 20 sperm following the addition of prog. Each row depicting the  $[Ca^{2+}]_i$  (upper) and membrane (lower) dynamics of a single cell over time. A white dotted line indicates the moment of addition. The images presented are representative of at least five independent experiments. Consistently, a  $[Ca^{2+}]_i$  transient precedes contraction, which is proportional to the increase in FM4-64 fluorescence, as shown in Figure S2D. E) Representative time series of  $[Ca^{2+}]_i$  and midpiece contraction dynamics. Capacitated CD1 sperm were loaded with Fluo4 AM, immobilized on concanavalin A-coated coverslips, and incubated in a recording medium containing 0.5  $\mu$ M FM4-64. AE was induced with 100  $\mu$ M progesterone (prog, arrowhead). Fluo4 images are widefield images, while FM4-64 images are SRRF-processed (super-resolution). Scale bar = 1  $\mu$ m. F) 3D kymographs of  $[Ca^{2+}]_i$  (left) and contraction (right) dynamics. Data are normalized to the mean of the frames before the induction of AE. Representative images from at least 5 independent experiments are shown, with 36 cells analyzed.

## The distance between the actin cytoskeleton and the plasma membrane is decreased during the contraction of the midpiece

The midpiece is shaped by two major structural elements: the axoneme, which consists of tubulin and its accessory components, including the outer dense fibers (ODFs); and a recently described network of filamentous actin (F-actin) arranged in a helicoidal conformation along the midpiece (13). We investigated whether the actin network plays a role in regulating the midpiece contraction associated with AE. We considered three possible scenarios: (i) an unknown mechanical force, mediated by a rigid matrix such as F-actin, brings the plasma membrane closer to the center of the flagellum; (ii) a dynamic relationship exists between the plasma membrane and the actin cytoskeleton of the midpiece, facilitating contraction; and (iii) the midpiece contraction is driven by an uncharacterized signaling mechanism that acts independently of the actin cytoskeleton.

The role of the actin cytoskeleton in the midpiece contraction was investigated through live-cell super-resolution using SiR-actin, a fluorescent probe that binds to F-actin (20–22). We used FM4-64 to visualize the plasma membrane (Figure 5) and transgenic sperm expressing DsRed2 to observe the mitochondrial network (Figure S4). Two stimulated sperm, one that experienced AE (Figure 5B) and another that did not (Figure 5A) are shown. In both cases, a network of F-actin was observed beneath the plasma membrane of the midpiece (cortical actin), enveloping the mitochondrial network (Figure S4A). As expected, in the absence of AE, the midpiece diameter (observed through FM4-64) remained unchanged (see also Figure 2, and Figure S4). In this case, both the diameter of the F-actin network and its proximity to either the plasma membrane or the mitochondrial network remained static (Figure 5A), suggesting a structural role for the F-actin network within the midpiece (scenario - (i)), such as supporting the organization of the mitochondrial network (Figure S4). Remarkably, acrosome-reacted sperm (Figure 5B) experienced an abrupt structural reorganization of the midpiece, characterized by a decrease in the distance between the plasma membrane and both the F-actin and mitochondrial networks (Figures S4 and S5). This observation suggests that the remodeling of the midpiece structure is driven by a mechanical (or molecular) interaction occurring at the boundaries of the plasma membrane (supporting scenario - (ii)).

To assess the potential interaction between the F-actin network and the plasma membrane (or its associated components), we examined their colocalization through live-cell super-resolution imaging. Figure 5C presents two Manders' colocalization coefficients (23). M1 represents the proportion of F-actin (in pixels) that colocalizes with the plasma membrane, while M2 measures the proportion of plasma membrane pixels colocalizing with the F-actin network. A Manders' value of 1 indicates full colocalization, while a value of 0 implies no colocalization.

Figure 5C reveals that acrosome-intact sperm displayed low Manders' coefficients ( $M1 = 0.32 \pm 0.03$ ;  $M2 = 0.28 \pm 0.04$ ). In contrast, sperm undergoing midpiece contraction exhibited a significant increase in colocalization between the F-actin network and the plasma membrane, as evidenced by the rise in M1 and M2 coefficients ( $M1 = 0.65 \pm 0.03$ ;  $M2 = 0.69 \pm 0.03$ ). This increased colocalization occurred simultaneously with midpiece contraction.

Overall, these results confirm that (i) the contraction of the midpiece is linked to the remodeling of the plasma membrane and potentially the F-actin cytoskeleton, and that (ii) both structures interact with each other, directly or indirectly, at the nanoscales. We then seek to understand whether the driving force for the contraction of the midpiece emanates from the F-actin network. The following scenarios were envisaged: (a) the plasma membrane moves towards the actin cytoskeleton, (b) the actin cytoskeleton moves towards the plasma membrane, or (c) both structures come closer to the center of the flagellum. To investigate the occurrence of any of these scenarios, the positions of fluorescence peaks of FM4-64 and SiR-actin in super-resolution

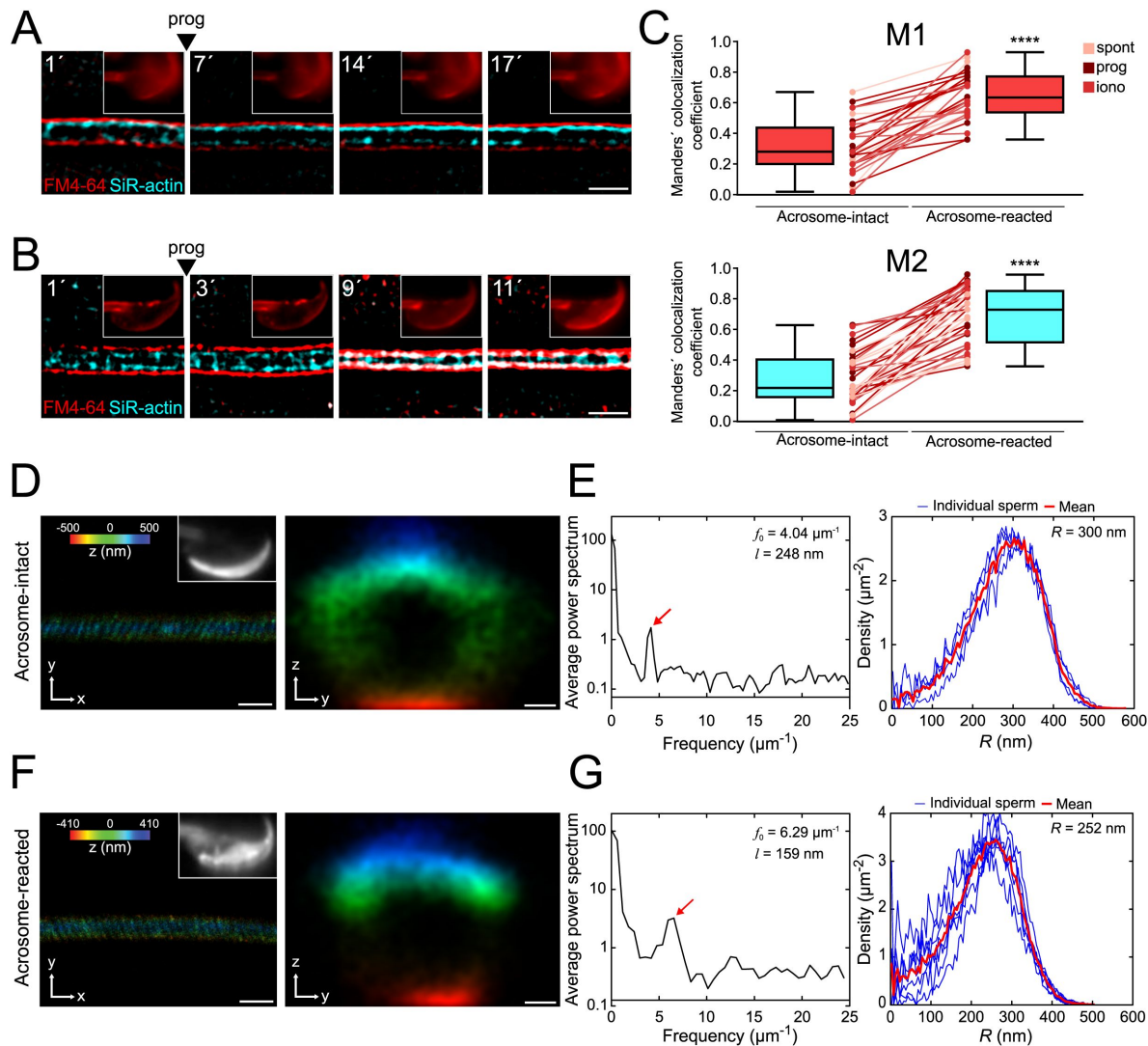


**Figure 5.**

### The flagellar membrane approaches the actin cytoskeleton in the midpiece of the sperm flagellum during midpiece contraction and AE.

A-B) Representative time series of plasma membrane and actin cytoskeleton colocalization in the midpiece in the absence of AE (A) and during progesterone-induced AE (B, prog, 100  $\mu\text{M}$ ; FM4-64 shown in red, SiR-actin shown in cyan). Capacitated CD1 sperm were loaded with 100 nM SiR-actin, immobilized on concanavalin A-coated coverslips, and incubated in a recording medium containing 0.5  $\mu\text{M}$  FM4-64. Scale bar = 1  $\mu\text{m}$ . Representative images from at least 5 independent experiments are shown, with 36 cells analyzed. C) Manders' colocalization coefficients for acrosome-intact and acrosome-reacted cells in the midpiece. M1 was assigned to FM4-64, and M2 to SiR-actin. Data are presented as mean  $\pm$  SEM. \*\*\*\*p<0.0001 represents statistical significance. Paired t test was performed. D-G) Representative images of sperm midpiece stained with the acrosome marker PNA (left panel, upper right insets, epifluorescence) and phalloidin (actin filaments, STORM) for acrosome-intact (D-E) and acrosome-reacted (F-G) cells. The left panel displays a longitudinal section of the midpiece (Scale bar = 10  $\mu\text{m}$ ), while the right panel illustrates the radial distribution (Scale bar = 0.2  $\mu\text{m}$ ). E and G) Schematics of the analyzed actin double helix parameters in the midpiece: helical pitch ( $l$ , distance between turns of the helix, left panel), helical pitch frequency ( $f_0$ , number of turns the helix makes per 1  $\mu\text{m}$ ), and radial distribution ( $R$ , radius of the double helix, right panel). Representative images from at least 3 independent experiments are shown. Four acrosome-intact cells and seven acrosome-reacted cells were analyzed.

kymographs were tracked, as proxy of either membrane or actin cytoskeleton localization, respectively (Figures S5A and S5B). Figure S5C shows representative histograms of SiR-actin and FM4-64 over time. Both FM4-64 and SiR-actin fluorescence peaks came closer to each other. This effect can be also seen in Figure S5F, where acrosome-intact cells display a distance of  $0.180 \pm 0.007 \mu\text{m}$  between the plasma membrane and the actin cytoskeleton. In acrosome-reacted cells, the distance was as small as  $0.074 \pm 0.006 \mu\text{m}$  after midpiece contraction.

In Figure S5D, a section of the midpiece of an ionomycin-induced AE sperm is shown. In this case, the plasma membrane and the actin cytoskeleton approach move closer toward the center of the cell. (set to 0). The slope calculated from the linear fit denotes the velocity of this change. In this example, the plasma membrane is contracting at a rate of  $14 \mu\text{m}/\text{min}$ , whereas the actin cytoskeleton is contracting at a rate of  $3 \mu\text{m}/\text{min}$  (Figure S5E). In both cases, the signal presents a negative slope in sperm that underwent AE, consistent with a decrease in midpiece diameter. Since the results of the analysis of SiR-actin slopes were not conclusive, we studied the actin cytoskeleton structure in more detail.

## The actin cytoskeleton in the midpiece is remodeled during the AE

In the midpiece, polymerized actin forms a double helix that accompanies mitochondria (13). To investigate if the contraction of the midpiece is associated with structural modifications of the actin double-helix, 3D-STORM was used. Cells were exposed to progesterone, fixed, and co-stained with PNA and phalloidin to visualize the acrosomal status and the actin structure, respectively.

Figures 5D and 5F show representative images of both dyes for acrosome-intact and acrosome-reacted sperm (left panels). Different parameters were calculated: 1) Helical pitch ( $l$ ), which is the distance between turns of the helix; 2) Frequency ( $f_0 = 1/l$ ), obtained from the Fourier transform of the image and represented the number of turns that the helix makes per unit length; and 3) Radial distribution ( $R$ ), to infer the distance between the center of the midpiece and the maximum of fluorescence (13). The frequency increased substantially in the acrosome-reacted sperm compared to intact sperm ( $6.29$  vs  $4.04 \mu\text{m}^{-1}$ , Figures 5E and 5G, red arrows in left panels). In addition, the helical pitch diminished its magnitude in acrosome-reacted sperm ( $159$  nm vs  $248$  nm) (Figures 5E and 5G, left panels). The radial distribution of F-actin in cells that underwent AE indicated a smaller radius compared to acrosome-intact sperm ( $252$  vs  $300$  nm, Figures 5E and 5G, right panel). Altogether, these results confirm that the actin double-helix undergoes structural changes during the contraction of the midpiece

To further investigate the structural rearrangements of the actin cytoskeleton during AE, a fluorescent molecule number and brightness analysis was performed (24–26). The number measure indicates the abundance or concentration of SiR-Actin molecules bound to F-actin fibers, while the brightness analysis helps reveal dynamic changes in molecular aggregation processes. This analysis is based on the idea that higher-order fluorescent complexes, which are mobile within the sample, will cause an increase in signal variability over time. An increase in brightness suggests the formation or movement of supramolecular structures, such as bundles of actin fibers bearing SiR-Actin. AE induction with progesterone and ionomycin resulted in a significant increase in actin number and brightness compared to the control (non-reacted) group (Figure S6A). Spontaneously reacted sperm also exhibited this behavior, albeit in a more moderate fashion (Figure S6A).

The observed increase in SiR-Actin number after AE induction suggests major actin monomer recruitment to the polymerizing fibers (Figure S6A and S6B), which produces an apparent increase in local fluorophore concentration (Figure S6B). This effect positively correlated with a similar increase in SiR-actin fluorescence (Figure S6A), which is known to indicate actin polymerization due to its high affinity for F-actin.



Actin cytoskeleton polymerization in the midpiece results in a signal variation of increased magnitude (an increase in SiR-Actin brightness) as it undergoes structural rearrangements (Figures S6A and S6B), which are compatible with other observations reported in this work. Both assembly and transport of actin complexes into higher oligomeric states (F-actin) across the cellular milieu led to an apparent increase in the registered SiR-Actin brightness (Figure S6B). Additionally, actin filament displacement along the mitochondrial sheath during AE provides a SiR-Actin brightness measure with high dispersion, indicating a redistribution of this cellular structure. These results suggest that actin filaments are locally redistributed and remodeled during AE (Figure S6B).

## Midpiece contraction in sperm located within the perivitelline space

In mice, only sperm undergoing AE prior to binding to the zona pellucida can penetrate and fertilize (27). We hypothesized that midpiece changes and motility cessation occur only after acrosome-reacted sperm penetrate the zona pellucida. Live imaging was performed after *in vitro* fertilization (IVF) using transgenic EGFP-DsRed2 sperm loaded with FM4-64. Eggs were inseminated with a high sperm count (200,000 cells) to increase the number of cells observed.

**Figure 6A** and Supplementary movie S7 show a sperm swimming within the perivitelline space. The FM4-64 fluorescence of this sperm midpiece is low (**Figure 6B**) which coincides with the fact that the sperm is moving (see also **Figure 1F-G**). Another example of this observation is shown in **Figure 6C-D**, an acrosome-reacted moving sperm within the perivitelline space had low FM4-64 fluorescence in the midpiece (**Figure 6C**). After 20 minutes, these sperm stopped moving and exhibited increased FM4-64 fluorescence, indicating midpiece contraction (**Figure 6D**). These results suggest that midpiece contraction and motility cessation occur after acrosome-reacted sperm penetrate the zona pellucida.

## Midpiece contraction takes place following sperm-egg fusion

Motile acrosome-reacted sperm, initially lacking midpiece contraction, can penetrate the zona pellucida. However, they eventually stop moving and exhibit an increase in FM4-64 fluorescence. This suggests that the cessation of motility plays a crucial role in fertilization events occurring after zona pellucida binding and penetration, and that a similar change in midpiece architecture is necessary for successful sperm-egg fusion. To explore this hypothesis, we designed a live imaging experiment using zona-free eggs. Denuded oocytes were loaded with Hoechst 33342, a nuclear dye, to visualize the exact moment of sperm-egg fusion (28–30). The experiment involved FM4-64, transgenic EGFP-DsRed2 sperm, and simultaneous signal collection from five separate channels (DIC, Hoechst, EGFP, DsRed2, and FM4-64). To enhance observation likelihood, volumetric data was collected by imaging at different z-planes (**Figure 7A**).

**Figure 7C** presents a representative volumetric time series of sperm-egg fusion, with only the optimal focal plane shown. The acrosome-reacted sperm (EGFP negative) initially did not display Hoechst fluorescence (Supplementary movie S8), indicating a lack of fusion. However, 14 minutes later, the dye entered the sperm and stained the nucleus, indicating fusion initiation. At this stage, sperm remain motile while bound to the egg plasma membrane. The midpiece diameter remained unchanged during initial sperm-egg fusion indicated by the low FM4-64 fluorescence. Following gamete fusion initiation, FM4-64 fluorescence increased (38 to 44 min), causing sperm motility to cease. In some instances, the midpiece folded and extended again (Figure S7B). These findings demonstrate that midpiece contraction occurs following sperm-egg fusion.



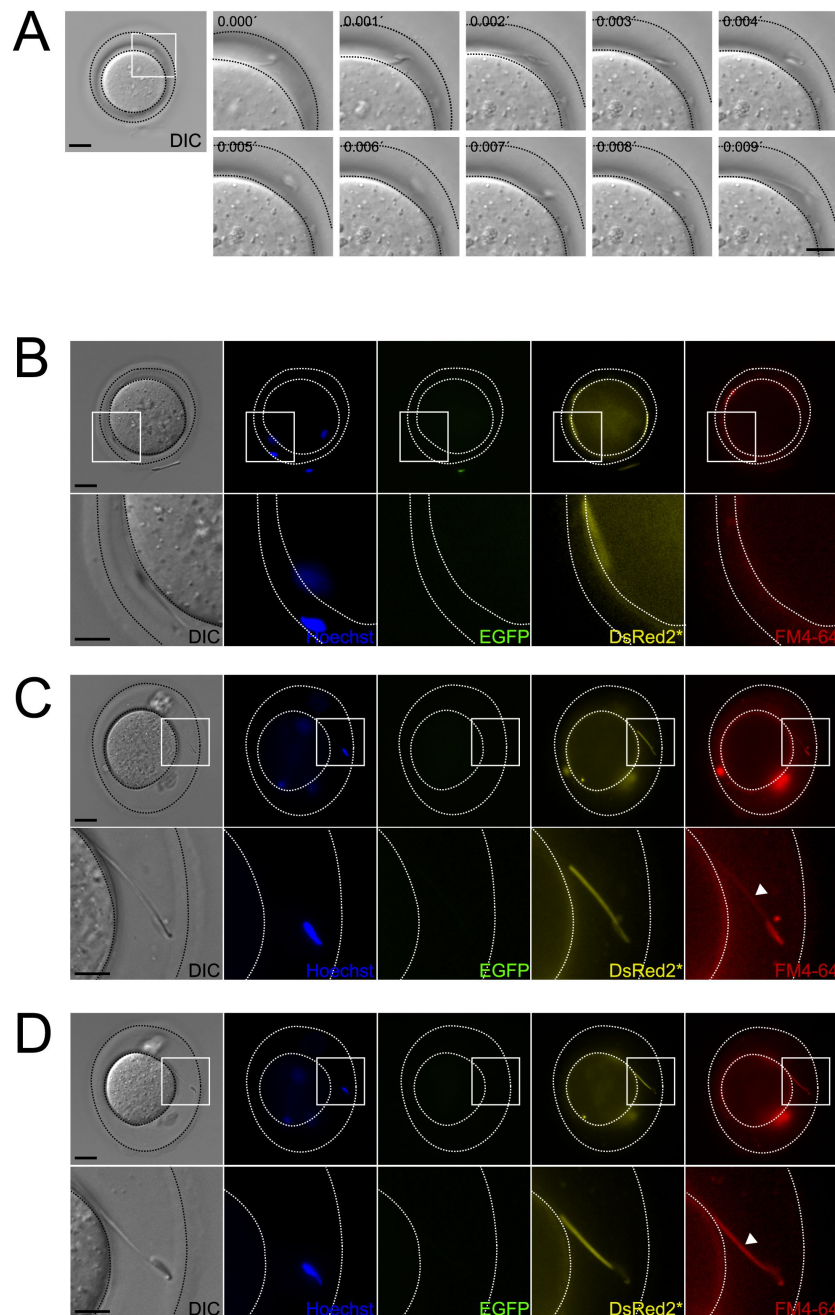


**Figure 6.**

### Occurrence of midpiece contraction in sperm located within the perivitelline space.

Representative images of IVF experiments using EGFP-DsRed2 sperm. Oocyte-sperm complexes were stained with 10  $\mu\text{g/ml}$  Hoechst and 10  $\mu\text{M}$  FM4-64. A) Representative time series of DIC images showing a sperm moving within the perivitelline space. Scale bar in right panel = 20  $\mu\text{m}$ , scale bar in left panel = 10  $\mu\text{m}$ . B) DIC, Hoechst, EGFP, DsRed2\*, and FM4-64 images are shown for the case depicted in [Figure 6A](#), note that, as the sperm is moving, it is located in a different position in the perivitelline space. The area depicted in the upper panel is shown in higher magnification in the lower panel. Scale bar in upper panel = 20  $\mu\text{m}$ , scale bar in lower panel = 10  $\mu\text{m}$ . C-D) DIC, Hoechst, EGFP, DsRed2\*, and FM4-64 images are shown for a (C) sperm that have passed through the ZP, displaying AE with an initially non-contracted midpiece. After 20 minutes, as shown in (D), the midpiece becomes contracted. The area depicted in the upper panel is shown in higher magnification in the lower panel. Scale bar in upper panel = 20  $\mu\text{m}$ , scale bar in lower panel = 10  $\mu\text{m}$ . Representative images from at least 6 independent experiments are shown. A total of 23 oocytes and 69 sperm were analyzed.

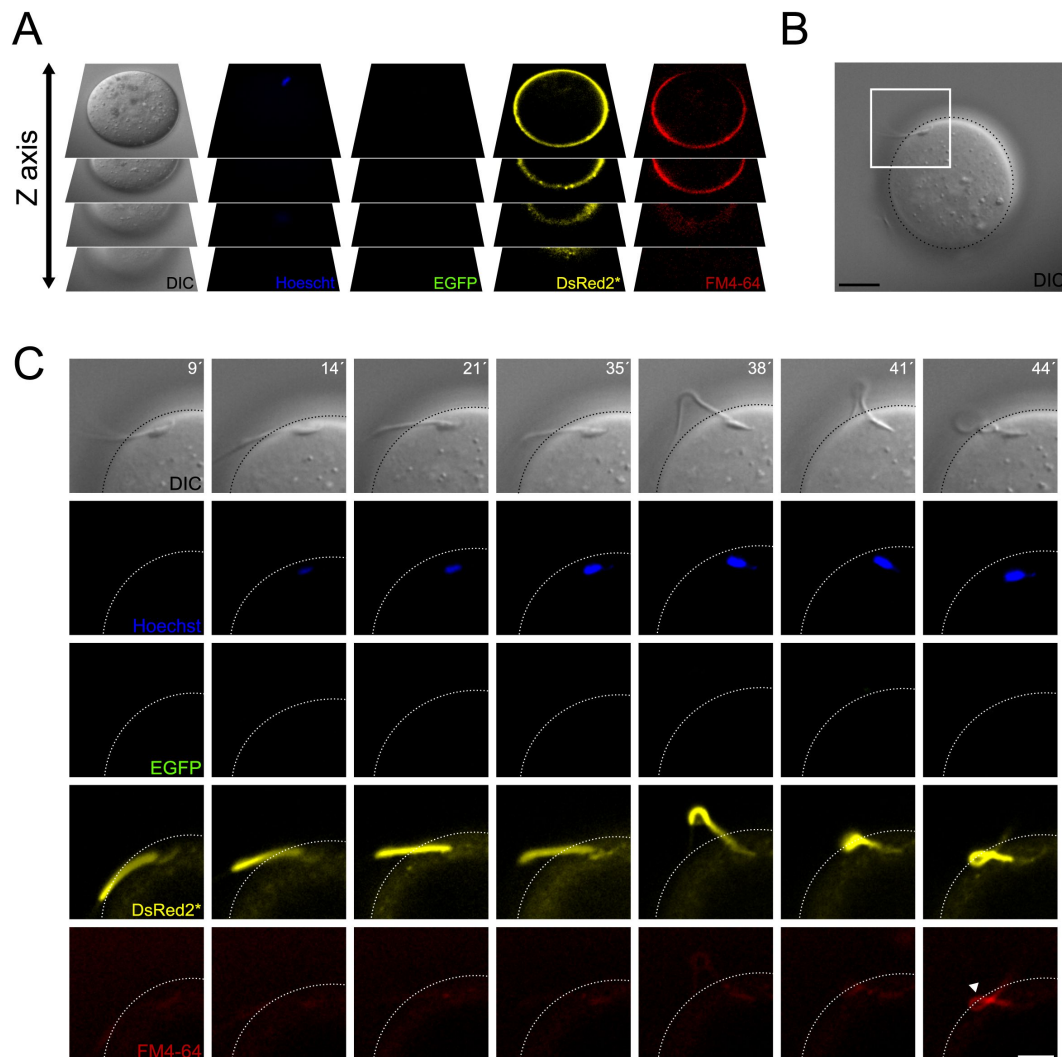


**Figure 7.**

**Contraction of the midpiece occurs after sperm-egg fusion.**

A) Schematic representation of the acquisition settings for the sperm-oocyte fusion assay. Images were taken every 7  $\mu\text{m}$  along the z-axis. B) DIC image of a sperm-oocyte complex, with the area depicted in higher magnification in panel C. Scale bar = 20  $\mu\text{m}$ . C) Representative time series of sperm-oocyte fusion assay experiments using EGFP-DsRed2 sperm. Oocytes were stained with 1  $\mu\text{g}/\text{ml}$  Hoechst and 10  $\mu\text{M}$  FM4-64. DIC, Hoechst, EGFP, DsRed2\*, and FM4-64 images are shown over time. Scale bar = 10  $\mu\text{m}$ . Note that midpiece contraction occurs after sperm-egg fusion and is proportional to the increase in FM4-64 fluorescence, as shown in Figure S2D, highlighting its potential importance in the fertilization process. Representative images from at least 4 independent experiments are displayed.

## A decrease in $[Ca^{2+}]_i$ in the midpiece following fusion precedes the midpiece contraction

In previous experiments, an increase in  $[Ca^{2+}]_i$  was observed throughout the midpiece, coinciding with midpiece contraction (Figure 4 and Figure S3). To examine the mechanism behind midpiece contraction after fusion, wild-type sperm loaded with Fluo4 were exposed to denuded oocytes loaded with Hoechst. We hypothesized that dynamic changes in  $[Ca^{2+}]_i$  during gamete fusion drive the midpiece contraction during sperm immobilization.

Figure 8A presents representative images from a time course live imaging experiment designed to observe sperm-egg fusion. The experiment involved simultaneous signal collection from four separate channels over time (DIC, Hoechst, Fluo4, and FM4-64). To enhance observation likelihood, images were taken at different z-planes, though only the optimal focal plane is shown.

Unexpectedly, sperm binding to the egg plasma membrane displayed high levels of  $[Ca^{2+}]_i$  in the head and midpiece (Figure 8A, time 1 min, and Supplementary movie S9). A few minutes after fusion began (indicated by an increase in Hoechst signal in the sperm), a decrease in  $[Ca^{2+}]_i$  in the head and midpiece was observed (21 min to 51 min). This decrease in  $[Ca^{2+}]_i$  was followed by midpiece contraction, as evidenced by the increase in FM4-64 fluorescence (56 min). In several cells, the midpiece folded back before contracting. The gametes that underwent this change in the flagellum typically remained folded, but occasionally the tail unfolded again. Figures 8B-F quantify the key events described above during sperm-egg fusion.

In summary,  $75.88 \pm 12.20$  % of the sperm exhibited midpiece contraction upon fusion. In  $61.83 \pm 12.04$  % of cases, the midpiece folded on itself, and afterward, only  $31.60 \pm 7.47$  % unfolded and stretched out again. All sperm bound to the plasma membrane before fusion presented high  $[Ca^{2+}]_i$  in the head, and the majority displayed a decrease in head  $[Ca^{2+}]_i$  before midpiece contraction ( $75.13 \pm 3.05$  %). Concerning the midpiece, three patterns were observed during fusion: in the majority of cases ( $69.67 \pm 11.46$  %), the midpiece experienced a decrease in  $[Ca^{2+}]_i$ . Additionally,  $10.33 \pm 10.33$  % of sperm showed a transient increase in  $[Ca^{2+}]_i$ , while the remaining  $20.00 \pm 9.41$  % displayed no changes.

Collectively, these results indicate that a decrease in  $[Ca^{2+}]_i$  in the midpiece after fusion precedes midpiece contraction and the cessation of sperm motility that precedes sperm-egg fusion.

## Discussion

In this article, we demonstrate the existence of a fundamental structural change that occurs in the sperm flagellum at the time of fusion with the egg. Using a plethora of advanced microscopy methods and single cell imaging, we provide insight about cellular and molecular events that occur in acrosome-reacted sperm, which, undoubtedly, are the ones capable of fertilizing an oocyte (2, 3). At this precise moment of the fertilization process, sperm need to stop moving to complete the fusion between the two gametes. The cease of movement is caused by two concomitant processes that take place in the flagellar midpiece region: a change in the F-actin helical structure and a decrease in the midpiece diameter. To the best of our knowledge, this is the first time that a structural modification of the sperm flagellum related to a specific cellular necessity, i.e., gamete fusion, is described.

To arrive at the site of fertilization within the female reproductive tract, sperm motility is required. It is also fundamental to penetrate the different layers surrounding the egg. In this journey, sperm sense the environment and adapt their movement to the different physiological

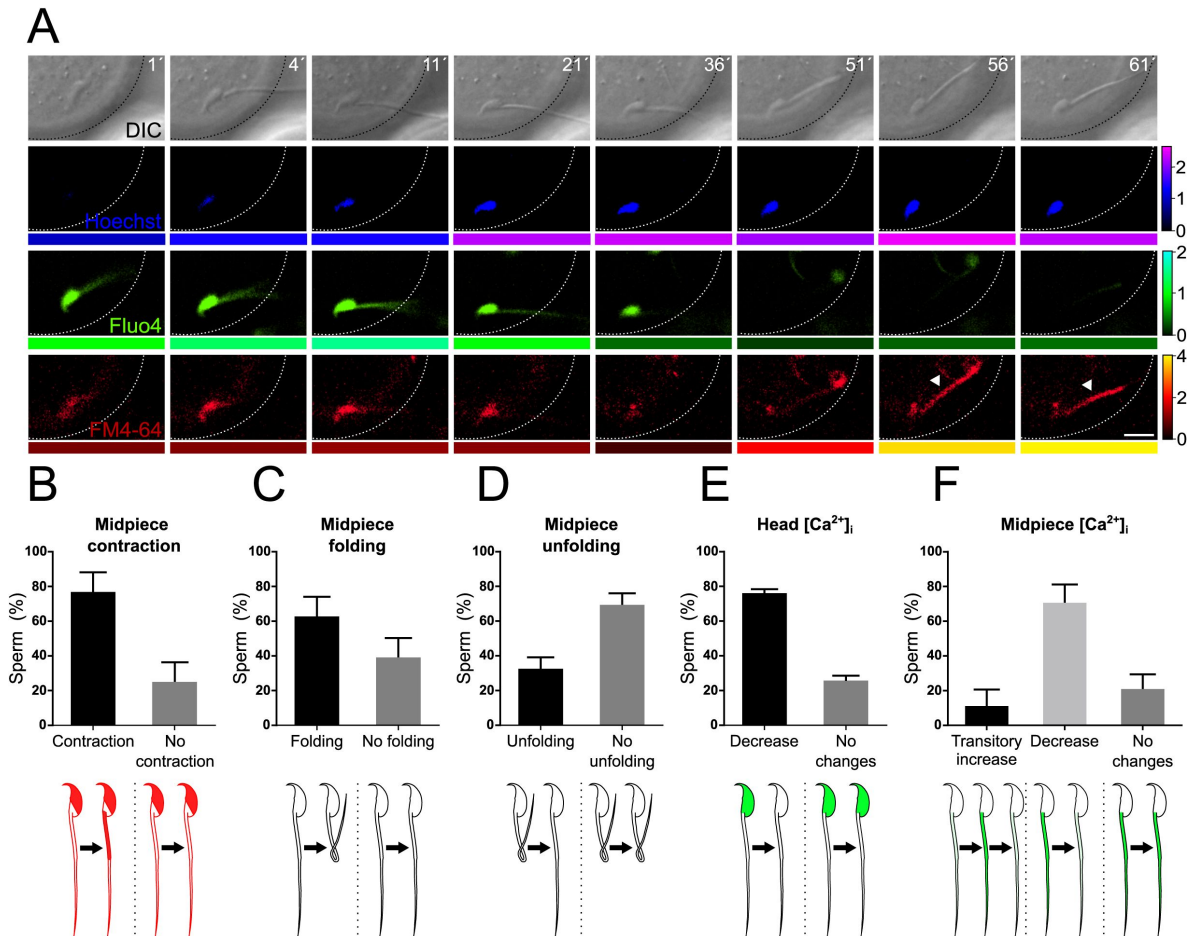


**Figure 8.**

### Midpiece contraction occurs in sperm-egg fusion after a decrease in $[Ca^{2+}]_i$ .

A) Representative time series of sperm-oocyte fusion assay experiments using wild-type sperm loaded with 1  $\mu$ M Fluo-4. Oocytes were stained with 1  $\mu$ g/ml Hoechst and 10  $\mu$ M FM4-64. DIC, Hoechst, Fluo-4, and FM4-64 images are shown over time. Scale bar = 10  $\mu$ m. The color code below each frame in the Hoechst (shown in blue), Fluo-4 (shown in green), and FM4-64 (shown in red) images indicates the normalized intensity of the fluorescence signal (scale bar on the right of the panel). B-F) Quantification of sperm showing midpiece contraction (B, indicated by increased FM4-64 fluorescence), midpiece folding (C), midpiece unfolding (D), Fluo-4 fluorescence dynamics in the head (E), and different patterns in the midpiece (F) during fusion. Data are presented as the mean  $\pm$  SEM of the percentage of sperm counted for each experiment. Representative images and data from at least 3 independent experiments are shown. A total of 74 oocytes and 136 sperm were analyzed. Note that midpiece contraction occurs in sperm-egg fusion after a decrease in Fluo-4 fluorescence.

scenarios. In addition, recent evidence also demonstrated that after being released from their site of storage in the oviductal isthmus, mouse sperm undergo AE (2, 3). This process occurs in the upper segments of the oviduct before any interaction with the eggs or their surrounding layers. This observation opened a new scenario about the motility of sperm in their last transit to the site of fertilization. Little is known about sperm in that region and how sperm move after AE. In this regard, most of the information about mammalian sperm comes from studies conducted *in vitro*, using a mixture of acrosome-intact and acrosome-reacted sperm. Even if their motility is analyzed in a subjective manner or using cell tracking systems, virtually all the experiments are conducted without discerning the acrosomal status of the cells. Another possible source of artifacts in this analysis is related with the fact that most of the experiments are also performed using epididymal sperm (not ejaculated) in aqueous solutions that support sperm capacitation but do not represent the natural viscous environment present in the female tract.

By performing *in vitro* experiments, we detected a strong association between the decrease in the midpiece diameter and the cease of sperm motility. This is observed in a subset of sperm after the occurrence of AE. This may suggest that only sperm that undergo AE in the oviduct and do not experience this midpiece contraction are capable of migrating to the ampulla and penetrate the cumulus and the zona pellucida. Those sperm that undergo this phenomenon earlier in the tract may not be suitable to continue their journey suggesting that this also may select the gametes during their transit to the ampulla. Previous observations tracking sperm within the female tract have shown the existence of acrosome-reacted sperm within the tract that remain non-motile (2–4).

Acrosome-reacted sperm that bind and penetrate the zona pellucida are ready to fuse with the egg. During sperm-egg fusion, several authors have reported in different species that sperm stop moving (7–9). However, the mechanism behind this behavior is not established. One possible explanation is that fusion promotes ion transport changes in sperm, which significantly alter flagellar movement. In this sense, it was previously demonstrated that certain ions such as  $\text{Ca}^{2+}$  may diffuse from the oocyte to the sperm (31). However, a clear technical limitation in our experimental approach is that the probes that monitor ion dynamics may be exchanged between both gametes. If the concentration of a given probe does not remain stable, it is impossible to determine the accurate change that occurs during fusion. Future experiments may take advantage of transgenic models that incorporate a particular sensor to study this process *in vivo*, such as the one used by Cohen and collaborators (32).

Regardless of the precise nature of ion exchange between sperm and eggs, the diameter of the sperm flagellum in the midpiece is reduced. This midpiece diameter reduction is strongly associated with cessation of sperm motility and is apparently needed to complete the fusion process. Our observation clearly supports this notion. Importantly, the sperm flagellum folds back during fusion coincident with the decrease in the midpiece diameter. Interestingly, this was previously observed in mammals as well as in sea urchin sperm (7, 33, 34).

Like other cylindrical biological structures, the sperm flagellum relies on the cytoskeleton for its structural organization and specialized mechanical properties. In addition to the change in midpiece diameter, a significant rearrangement of the F-actin cytoskeleton also occurs. In the midpiece, the polymerized actin is organized in a double helix accompanying the mitochondria (13). As in many other organisms, the actin cytoskeleton possesses important structural functions, and dynamic changes of F-actin allow the cells to conduct important cellular tasks such as exocytosis. However, less is known about the structural changes undergone by the actin cytoskeletons in cilia and flagella. Remarkably, it has been reported that actin forms helix-like structures in the flagellum of the parasite *Giardia intestinalis* (35). These findings open the question of whether, to some extent, flagellar helical structures are conserved among diverse species. Our observations demonstrate that the F-actin double helix undergoes a change in the helical pitch as well as in the radial distance to the axoneme. This is concomitant with the decrease



in midpiece diameter. Our single-cell experiments using super-resolution microscopy also revealed that the plasma membrane approached the F-actin network during this change. It is well established that various proteins can function as linkers between the plasma membrane and the actin cytoskeleton (36), but their roles in this specific process remain to be studied. Regardless of how these structures are connected, it is evident that both are associated. However, our experimental data cannot determine whether the plasma membrane is causing the change of the actin network or if the actin network influences the plasma membrane.

Another observation emerging from our study is that a change in  $[Ca^{2+}]_i$  occurs prior to the midpiece contraction. It is well known that  $Ca^{2+}$  is important for AE, and a specific transient rise in  $[Ca^{2+}]_i$  originating in the head can trigger exocytosis (19). Previous observations have demonstrated that the sperm head and tail are not isolated compartments, and that ions and other molecules can move between them (37, 38). In our single-cell experiments, we observed that the rise in FM4-64 fluorescence in the midpiece occurs after the increase in  $[Ca^{2+}]_i$  in that region, suggesting a potential association between these events. This could involve diffusion or active transport processes; further investigation is required to determine the precise mechanism to demonstrate if the structural changes are triggered by  $Ca^{2+}$ . In addition,  $[Ca^{2+}]_i$  increase and/or modification in the midpiece architecture may result in functional changes in the mitochondria such as the status of the mitochondrial membrane potential and the ATP production. This possibility needs to be further explored.

The same phenomenon was studied in sperm bound to the egg plasma membrane to evaluate if the rise in  $[Ca^{2+}]_i$  also occurs at the time of fusion. Remarkably, we noticed that most of the bound sperm that ended up fusing with the eggs displayed high levels of  $[Ca^{2+}]_i$  in both the head and the flagellum. The midpiece contraction and the immobilization occurred when the levels of  $[Ca^{2+}]_i$  went down in the midpiece suggesting a possible connection between both events. However, our experimental approach limits the interpretation of this result. One possible explanation is that as soon as sperm bind to the plasma membrane of the oocyte, there is a rapid increase in  $[Ca^{2+}]_i$  in the sperm. On the other hand, a massive transport of  $Ca^{2+}$  from the egg to the sperm could also occur. These hypotheses, however, are hindered by the technical limitations mentioned above. As the oocyte is not loaded with Fluo4, we cannot rule out that the apparent  $[Ca^{2+}]_i$  decrease seen in these experiments is due to dye diffusion into the oocyte. Either way, it is clear that the transport of this ion into or out of the sperm is key to cease motility at this fundamental step of fertilization (16). Additionally, these results demonstrate that only sperm with elevated  $[Ca^{2+}]_i$  are capable of binding to the eggs. All these possible scenarios need to be determined in future experiments. Thus, regardless of the mechanism, a clear change in  $[Ca^{2+}]_i$  dynamics is observed at the time of midpiece contraction. Future studies will aid to indicate if certain  $Ca^{2+}$ -dependent proteins that can modify the actin cytoskeleton are responsible for this change.

**Why sperm stop moving:** We propose three possible hypotheses. The cessation of sperm motility can be attributed to the simultaneous or not occurrence of various events. 1) a rapid increase in  $[Ca^{2+}]_i$  levels may trigger the activation of  $Ca^{2+}$  pumps within the flagellum. This process consumes local ATP levels, disrupting glycolysis in the process. 2) Reorganization of the actin cytoskeleton: alterations in the actin cytoskeleton can lead to changes in the mechanical properties of the flagellum, impacting its ability to move effectively. 3) Midpiece contraction: Contraction in the midpiece region can potentially interfere with mitochondrial function, thereby impeding the energy production necessary for sustained motility. In addition, we speculate that the folding of the flagellum during fusion further facilitates sperm immobilization because it makes it more difficult for the flagellum to beat. Such process can enhance stability and increase the probability of fusion success. Mechanistically, the folding may occur as a consequence of the deformation-induced stress that develops during the decrease of midpiece diameter.



In cilia, apart from the findings presented in this paper, nothing is known about the regulation of motility by actin. Actin has been found to participate in ciliogenesis, but its involvement in active motility regulation has not been reported. This highlights a potentially unique role for the actin cytoskeleton in regulating sperm function during fertilization. Our discovery of actin's dynamic reorganization in sperm suggests it could have a more active role in regulating motility and other functions. Given the conservation of cilia and flagella across various organisms, our discovery could prompt further research on the role of the actin network in these structures.

In conclusion, we demonstrate that sperm undergo a structural reorganization of the actin cytoskeleton during key events of fertilization, as summarized in the working model shown in **Figure 9** [↗](#). Our findings introduce a new aspect of study in reproductive biology. Previous research has mainly focused on identifying proteins essential for sperm-egg fusion. Our results reveal a previously unexplored biological mechanism in mammalian fertilization, opening new avenues for contraceptive method development.

## Materials and methods

Detailed methods and protocols are provided in the SI appendix. For sample details, optical equipment, imaging conditions and probes used, see Supplementary Table S1.

## Acknowledgements

We gratefully acknowledge the financial support provided by the Williams and Rene Baron Foundations, the Male Contraceptive Initiative (MCI), and the Chan-Zuckerberg Initiative (CZI) for this work. Our sincere thanks go to Dr. Pablo Visconti for his valuable insights throughout the course of this project. We also thank Yoloxochitl Sánchez-Guevara for her technical support. This paper is dedicated to the memory of OAP.

## Funding

This work was supported by: Chan Zuckerberg Initiative (2021-240504 to MB and AG, GBI-0000000093 to AG, 2022-252509 to AG); Agencia Nacional de Promoción Científica y Tecnológica (PICT, 2017-3047, 2018-1988 and 2020-00988); Dirección General de Asuntos del Personal Académico/Universidad Nacional Autónoma de México (DGAPA/UNAM grant: IN105222 to GK, IN211821 to AG and IN200919 to AD); National Institute of Health (R01HD380882 to AD, R01HD106968 to DK and MGB).

## Author contributions

Investigation: MJ, GML, MDGE, CSC, JLDLVB, AL, AAH, MPRG, ALS. Data curation: MJ and VXAA. Writing: MJ, MGB and AG. Methodology: XX, Diego K and GK. Conceptualization: Dario K, Diego K, AD, MGB and AG. Supervision: MGB and AG.

## Competing interests

The authors declare no competing interests.

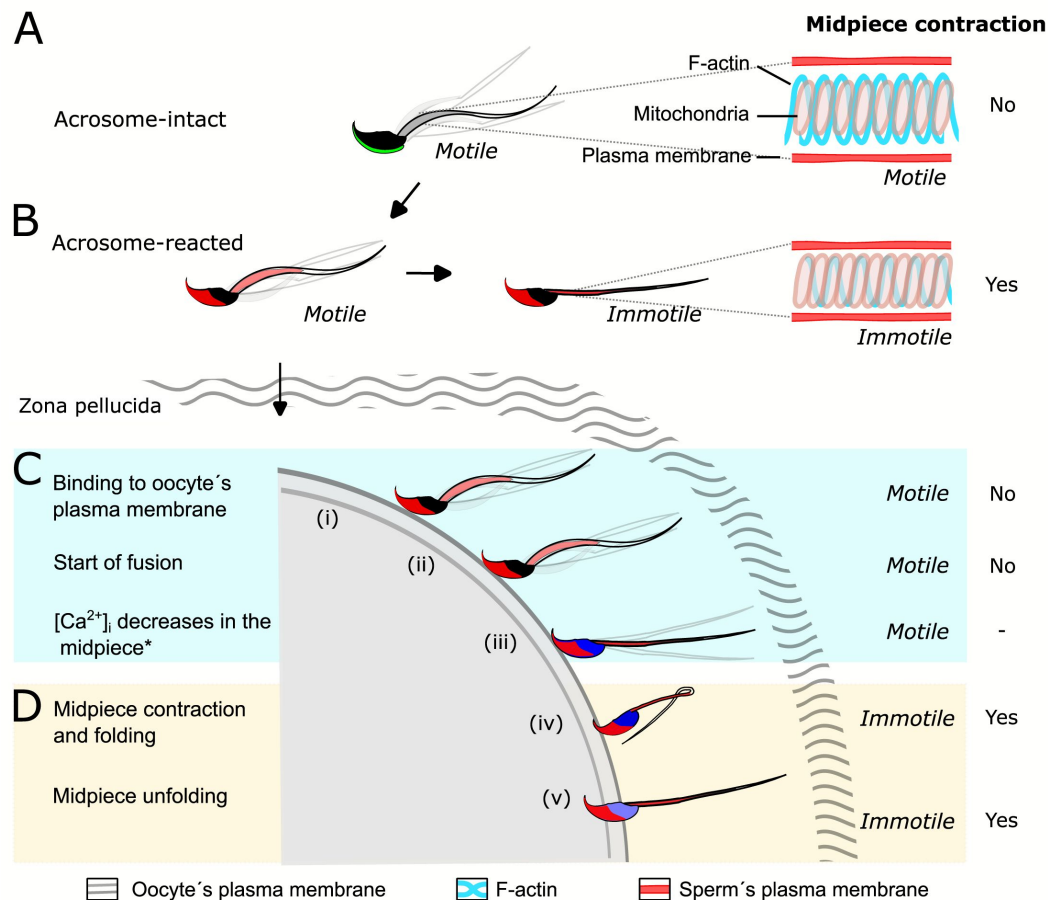


**Figure 9**

**Proposed model of the structural reorganization of the sperm actin cytoskeleton during key events of fertilization.**

The double helix actin network surrounding the mitochondrial sheath of the midpiece undergoes structural changes prior to the motility cessation. This structural modification is accompanied by a decrease in diameter of the midpiece and is driven by intracellular calcium changes that occur concomitant with a reorganization of the actin helicoidal cortex. Although midpiece contraction may occur in a subset of cells that undergo AE (A and B), the midpiece contraction occurs prior to motility cessation observed after sperm-egg fusion (C and D).

## Data, Materials, and Software Availability

Data acquired and analyzed during this study are included in this manuscript or will be available at Zenodo. Github will be used for depositing the code use in analysis.

## References

1. Demott R. P., Suarez S. S. (1992) **Hyperactivated sperm progress in the mouse oviduct** *Biol Reprod* **46**:779–785
2. Hino T., Muro Y., Tamura-Nakano M., Okabe M., Tateno H., Yanagimachi R. (2016) **The Behavior and Acrosomal Status of Mouse Spermatozoa In Vitro, and Within the Oviduct During Fertilization after Natural Mating** *Biol Reprod* **95**:50–50
3. La Spina F. A., Puga L. C., Romarowski A., Vitale A. M., Falzone T. L., Krapf D., Hirohashi N., Buffone M. G. (2016) **Mouse sperm begin to undergo AE in the upper isthmus of the oviduct** *Dev Biol* **411**:172–182
4. Muro Y., Hasuwa H., Isotani A., Miyata H., Yamagata K., Ikawa M., Yanagimachi R., Okabe M. (2016) **Behavior of Mouse Spermatozoa in the Female Reproductive Tract from Soon after Mating to the Beginning of Fertilization** *Biol Reprod* **94**:80–80
5. Inoue N., Ikawa M., Isotani A., Okabe M. (2005) **The immunoglobulin superfamily protein Izumo is required for sperm to fuse with eggs** *Nature* **434**:234–238
6. Noda T., Lu Y., Fujihara Y., Oura S., Koyano T., Kobayashi S., Matzuk M. M., Ikawa M. (2020) **Sperm proteins SOF1, TMEM95, and SPACA6 are required for sperm-oocyte fusion in mice** *Proc Natl Acad Sci U S A* **117**
7. Gaddum-Rosse P., Blandau R. J., Langley L. B., Battaglia D. E. (1984) **In vitro fertilization in the rat: observations on living eggs** *Fertil Steril* **42**:285–292
8. Gaddum-Rosse P., Blandau R. J., Langley L. B., Sato K. (1982) **Sperm tail entry into the mouse egg in vitro** *Gamete Res* **6**:215–223
9. Ravaux B., Garroum N., Perez E., Willaime H., Gourier C. (2016) **A specific flagellum beating mode for inducing fusion in mammalian fertilization and kinetics of sperm internalization** *Sci Rep* **6**
10. Deneke V. E., Pauli A. (2021) **The Fertilization Enigma: How Sperm and Egg Fuse** *Annu. Rev. Cell Dev. Biol* **37**:391–414
11. Siu K. K., Serrão V. H. B., Ziyat A., Lee J. E. (2021) **The cell biology of fertilization: Gamete attachment and fusion** *J Cell Biol* **220**
12. Otani H., Tanaka O., Kasai K., Yoshioka T. (1988) **Development of mitochondrial helical sheath in the middle piece of the mouse spermatid tail: regular dispositions and synchronized changes** *Anat Rec* **222**:26–33
13. Gervasi M. G., Xu X., Carbajal-Gonzalez B., Buffone M. G., Visconti P. E., Krapf D. (2018) **The actin cytoskeleton of the mouse sperm flagellum is organized in a helical structure** *J Cell Sci* **131**
14. Yanagimachi R. (1994) **Mammalian Fertilization**

15. Inaba K., Shiba K. (2018) **Microscopic analysis of sperm movement: links to mechanisms and protein components** *Microscopy* **67**:144–155
16. Sanchez-Cardenas C., Servin-Vences M. R., Jose O., Trevino C. L., Hernandez-Cruz A., Darszon A. (2014) **Acrosome Reaction and Ca<sup>2+</sup> Imaging in Single Human Spermatozoa: New Regulatory Roles of [Ca<sup>2+</sup>]<sub>i</sub>** *Biol Reprod* **91**:67–67
17. Gustafsson N., Culley S., Ashdown G., Owen D. M., Pereira P. M., Henriques R. (2016) **Fast live-cell conventional fluorophore nanoscopy with ImageJ through super-resolution radial fluctuations** *Nat Commun* **7**
18. Torres-García E. *et al.* (2022) **Extending resolution within a single imaging frame** *Nature Communications* **13**:1–22
19. Romarowski A. *et al.* (2016) **A Specific Transitory Increase in Intracellular Calcium Induced by Progesterone Promotes AE in Mouse Sperm** *Biol Reprod* **94**:1–12
20. Lukinavičius G. *et al.* (2014) **Fluorogenic probes for live-cell imaging of the cytoskeleton** *Nature Methods* **11**:731–733
21. Magliocca V., Petrini S., Franchin T., Borghi R., Niceforo A., Abbaszadeh Z., Bertini E., Compagnucci C. (2017) **Identifying the dynamics of actin and tubulin polymerization in iPSCs and in iPSC-derived neurons** *Oncotarget* **8**:111096–111109
22. Yamazaki S., Harata M., Idehara T., Konagaya K., Yokoyama G., Hoshina H., Ogawa Y. (2018) **Actin polymerization is activated by terahertz irradiation** *Sci Rep* **8**
23. Dunn K. W., Kamocka M. M., McDonald J. H. (2011) **A practical guide to evaluating colocalization in biological microscopy** *Am J Physiol Cell Physiol* **300**
24. Digman M. A., Dalal R., Horwitz A. F., Gratton E. (2008) **Mapping the Number of Molecules and Brightness in the Laser Scanning Microscope** *Biophys J* **94**
25. Mandracchia B., Hua X., Guo C., Son J., Urner T., Jia S. (2020) **Fast and accurate sCMOS noise correction for fluorescence microscopy** *Nat Commun* **11**
26. Liu S., Mlodzianoski M. J., Hu Z., Ren Y., McElmurry K., Suter D. M., Huang F. (2017) **sCMOS noise-correction algorithm for microscopy images** *Nature Methods* **14**:760–761
27. Jin M., Fujiwara E., Kakiuchi Y., Okabe M., Satouh Y., Baba S. A., Chiba K., Hirohashi N. (2011) **Most fertilizing mouse spermatozoa begin their acrosome reaction before contact with the zona pellucida during in vitro fertilization** *Proc Natl Acad Sci U S A* **108**:4892–4896
28. Conover J. C., Gwatkin R. B. L. (1988) **Pre-loading of mouse oocytes with DNA-specific fluorochrome (Hoechst 33342) permits rapid detection of sperm-oocyte fusion** *J Reprod Fertil* **82**:681–690
29. Hinkley R. E., Wright B. D., Lynn J. W. (1986) **Rapid visual detection of sperm-egg fusion using the DNA-specific fluorochrome Hoechst 33342** *Dev Biol* **118**:148–154
30. Stewart-Savage J., Bavister B. D. (1988) **A cell surface block to polyspermy occurs in golden hamster eggs** *Dev Biol* **128**:150–157

31. Jones K. T., Soeller C., Cannell M. B. (1998) **The passage of Ca<sup>2+</sup> and fluorescent markers between the sperm and egg after fusion in the mouse** *Development* **125**:4627–4635
32. Cohen R., Mukai C., Nelson J. L., Zenilman S. S., Sosnicki D. M., Travis A. J. (2022) **A genetically targeted sensor reveals spatial and temporal dynamics of acrosomal calcium and sperm acrosome exocytosis** *Journal of Biological Chemistry* **298**:101868–101869
33. Darszon A., Guerrero A., Galindo B. E., Nishigaki T., Wood C. D. (2004) **Sperm-activating peptides in the regulation of ion fluxes, signal transduction and motility** *International Journal of Developmental Biology* **52**:595–606
34. Guerrero A., Nishigaki T., Carneiro J., Tatsu Yoshiro, Wood C. D., Darszon A. (2010) **Tuning sperm chemotaxis by calcium burst timing** *Dev Biol* **344**:52–65
35. Paredeza A. R., Assafa Z. J., Sept D., Timofejeva L., Dawson S. C., Wang C. J. R., Cande W. Z. (2011) **An actin cytoskeleton with evolutionarily conserved functions in the absence of canonical actin-binding proteins** *Proc Natl Acad Sci U S A* **108**:6151–6156
36. Köster D. V., Mayor S. (2016) **Cortical actin and the plasma membrane: inextricably intertwined** *Curr Opin Cell Biol* **38**:81–89
37. Buffone M. G., Ijiri T. W., Cao W., Merdushev T., Aghajanian H. K., Gerton G. L. (2013) **Heads or Tails? Structural events and molecular mechanisms that promote mammalian sperm AE and motility** *Molecular Reproduction* **79**:4–18
38. De La Vega-Beltran J. L., Sánchez-Cárdenas C., Krapf D., Hernandez-González E. O., Wertheimer E., Treviño C. L., Visconti P. E., Darszon A. (2012) **Mouse sperm membrane potential hyperpolarization is necessary and sufficient to prepare sperm for the acrosome reaction** *Journal of Biological Chemistry* **287**:44384–44393
39. Hasuwa H., Muro Y., Ikawa M., Kato N., Tsujimoto Y., Okabe M. (2010) **Transgenic Mouse Sperm that Have Green Acrosome and Red Mitochondria Allow Visualization of Sperm and Their Acrosome Reaction in Vivo** *Exp. Anim* **59**:105–107
40. Corkidi G., Hernandez-Herrera P., Montoya F., Gadêlha H., Darszon A. (2021) **Long-term segmentation-free assessment of head-flagellum movement and intracellular calcium in swimming human sperm** *J Cell Sci* **134**
41. Culley S., Tosheva K. L., Matos Pereira P., Henriques R. (2018) **SRRF: Universal live-cell super-resolution microscopy** *Int J Biochem Cell Biol* **101**:74–79
42. Campagnola G., Nepal K., Schroder B. W., Peersen O. B., Krapf D. (2015) **Superdiffusive motion of membrane-targeting C2 domains** *Sci Rep* **5**
43. Weigel A. V., Simon B., Tamkun M. M., Krapf D. (2011) **Ergodic and nonergodic processes coexist in the plasma membrane as observed by single-molecule tracking** *Proceedings of the National Academy of Sciences* **108**:6438–6443
44. Izeddin I., El Beheiry M., Andilla J., Ciepielewski D., Darzacq X., Dahan M. (2012) **PSF shaping using adaptive optics for three-dimensional single-molecule super-resolution imaging and tracking** *Opt Express* **20**
45. Huang B., Wang W., Bates M., Zhuang X. (2008) **Three-dimensional super-resolution imaging by stochastic optical reconstruction microscopy** *Science* **319**:810–3



46. Ovesný M., Křížek P., Borkovec J., Švindrych Z., Hagen G. M. (2014) **ThunderSTORM: a comprehensive ImageJ plug-in for PALM and STORM data analysis and super-resolution imaging** *Bioinformatics* **30**:2389–2390
47. Luque G. M. *et al.* (2021) **Cdc42 localized in the CatSper signaling complex regulates cAMP-dependent pathways in mouse sperm** *The FASEB Journal* **35**
48. Stival C. *et al.* (2018) **Disruption of protein kinase A localization induces AE in capacitated mouse sperm** *Journal of Biological Chemistry* **293**:9435–9447
49. Nicolson G. L., Yanagimachi R., Yanagimachi H. (1975) **Ultrastructural localization of lectin-binding sites on the zonae pellucidae and plasma membranes of mammalian eggs** *J Cell Biol* **66**:263–274

## Editors

Reviewing Editor

**Jean-Ju Chung**

Yale University, New Haven, United States of America

Senior Editor

**Wei Yan**

The Lundquist Institute, Torrance, United States of America

### Reviewer #2 (Public Review):

Summary:

The authors used state-of-the-art microscopy to analyze the structural changes that occur in sperm tails after the acrosome reaction. They found that midpiece contraction and actin reorganization occurred, which is associated with the cessation of flagellar motility during sperm-egg fusion. The mechanism by which flagellar motility is arrested during sperm-oocyte fusion is unknown, and this study proposes its novel mechanism and provides important insights for cell and reproductive biologists.

In the revised manuscript, the authors addressed most of my concerns.

Strength:

Various microscopy techniques including super-resolution microscopy and scanning electron microscopy were used to analyze structural organization of the midpiece in detail.

<https://doi.org/10.7554/eLife.93792.2.sa2>

### Reviewer #3 (Public Review):

While progressive and also hyperactivated motility are required for sperm to reach the site of fertilization and to penetrate oocyte's outer vestments, during fusion with the oocyte's plasma membrane it has been observed that sperm motility ceases. Identifying the underlying molecular mechanisms would provide novel insights into a crucial but mostly overlooked physiological change during the sperm's life cycle. In this publication the authors aim to provide evidence that the helical actin structure surrounding the sperm mitochondria in the midpiece plays a role in regulating sperm motility, specifically the motility arrest during

sperm fusion but also during earlier cessation of motility in a subpopulation of sperm post acrosomal exocytosis.

The main observation the authors make is that in a subpopulation of sperm undergoing acrosomal exocytosis and sperm that fuse with the plasma membrane of the oocyte display a decrease in midpiece parameter of 30 nm. The authors propose the decrease in midpiece diameter via various microscopy techniques based on membrane dyes and bright-field images. In the revised version of the manuscript, a change in midpiece diameter is now confirmed via electron microscopy, even though the difference is not significant. The authors also propose that the midpiece diameter decrease is driven by changes in sperm intracellular  $\text{Ca}^{2+}$  and structural changes of the actin helix network. Future studies are still needed to confirm the casualty of these events and explore the discrepancy between fluorescence microscopy results and SEM. Overall, the authors should further tone down their conclusions.

<https://doi.org/10.7554/eLife.93792.2.sa1>

### Author response:

The following is the authors' response to the original reviews.

#### **Reviewer #1 (Public Review):**

##### *Summary:*

*This important work advances our understanding of sperm motility regulation during fertilization by uncovering the midpiece/mitochondria contraction associated with motility cessation and structural changes in the midpiece actin network as its mode of action. The evidence supporting the conclusion is solid, with rigorous live cell imaging using state-of-the-art microscopy, although more functional analysis of the midpiece/mitochondria contraction would have further strengthened the study. The work will be of broad interest to cell biologists working on the cytoskeleton, mitochondria, cell fusion, and fertilization. Strengths: The authors demonstrate that structural changes in the flagellar midpiece F-actin network are concomitant to midpiece/mitochondrial contraction and motility arrest during sperm-egg fusion by rigorous live cell imaging using state-of-art microscopy.*

Response P1.1: We thank the reviewer for her/his positive assessment of our manuscript.

##### *Weaknesses:*

*Many interesting observations are listed as correlated or in time series but do not necessarily demonstrate the causality and it remains to be further tested whether the sperm undergoing midpiece contraction are those that fertilize or those that are not selected. Further elaboration of the function of the midpiece contraction associated with motility cessation (a major key discovery of the manuscript) would benefit from a more mechanistic study.*

Response P1.2: We thank the reviewer for this point. We have toned down some of our statements since some of the observations are indeed temporal correlations. We will explore some of these possible connections in future experiments. In addition, we have now incorporated additional experiments and possible explanations about the function of the midpiece contraction.

**Reviewer #2 (Public Review):**

*(1) The authors used various microscopy techniques, including super-resolution microscopy, to observe the changes that occur in the midpiece of mouse sperm flagella. Previously, it was shown that actin filaments form a double helix in the midpiece. This study reveals that the structure of these actin filaments changes after the acrosome reaction and before sperm-egg fusion, resulting in a thinner midpiece. Furthermore, by combining midpiece structure observation with calcium imaging, the authors show that changes in intracellular calcium concentrations precede structural changes in the midpiece. The cessation of sperm motility by these changes may be important for fusion with the egg. Elucidation of the structural changes in the midpiece could lead to a better understanding of fertilization and the etiology of male infertility. The conclusions of this manuscript are largely supported by the data, but there are several areas for improvement in data analysis and interpretation. Please see the major points below.*

Response P2.1: We thank the reviewer for the positive comments.

*(2) It is unclear whether an increased FM4-64 signal in the midpiece precedes the arrest of sperm motility. in or This needs to be clarified to argue that structural changes in the midpiece cause sperm motility arrest. The authors should analyze changes in both motility and FM4-64 signal over time for individual sperm.*

Response P2.2 : We have conducted single cell experiments tracking both FM4-64 and motility as the reviewer suggested (Supplementary Fig S1). We have observed that in all cases, cells gradually diminished the beating frequency and increased FM4-64 fluorescence in the midpiece until a complete motility arrest is observed. A representative example is shown in this Figure but we will reinforce this concept in the results section.

*(3) It is possible that sperm stop moving because they die. Figure 1G shows that the FM464 signal is increased in the midpiece of immotile sperm, but it is necessary to show that the FM4-64 signal is increased in sperm that are not dead and retain plasma membrane integrity by checking sperm viability with propidium iodide or other means.*

Response P2.3: This is a very good point. In our experiments, we always considered sperm that were motile to hypothesize about the relevance of this observation. We have two types of experiments:

(1) Sperm-egg Fusion: In experiments where sperm and eggs were imaged to observe their fusion, sperm were initially moving and after fusion, the midpiece contraction (increase in FM4-64 fluorescence was observed) indicating that the change in the midpiece (that was observed consistently in all fusing cells analyzed), is part of the process.

(2) Sperm that underwent acrosomal exocytosis (AE): we have observed two behaviours as shown in Figure 1:

a) Sperm that underwent AE and they remain motile without midpiece contraction (they are alive for sure);

b) Sperm that underwent AE and stopped moving with an increase in FM464 fluorescence. We propose that this contraction during AE is not desired because it will impede sperm from moving forward to the fertilization site when they are in the female reproductive tract. In this case, we acknowledge that the cessation of sperm motility may be attributed to cellular death, potentially correlating with the increased FM4-64 signal observed in the midpiece of immotile sperm that have undergone AE. To address this hypothesis, we conducted image-

based flow cytometry experiments, which are well-suited for assessing cellular heterogeneity within large populations.

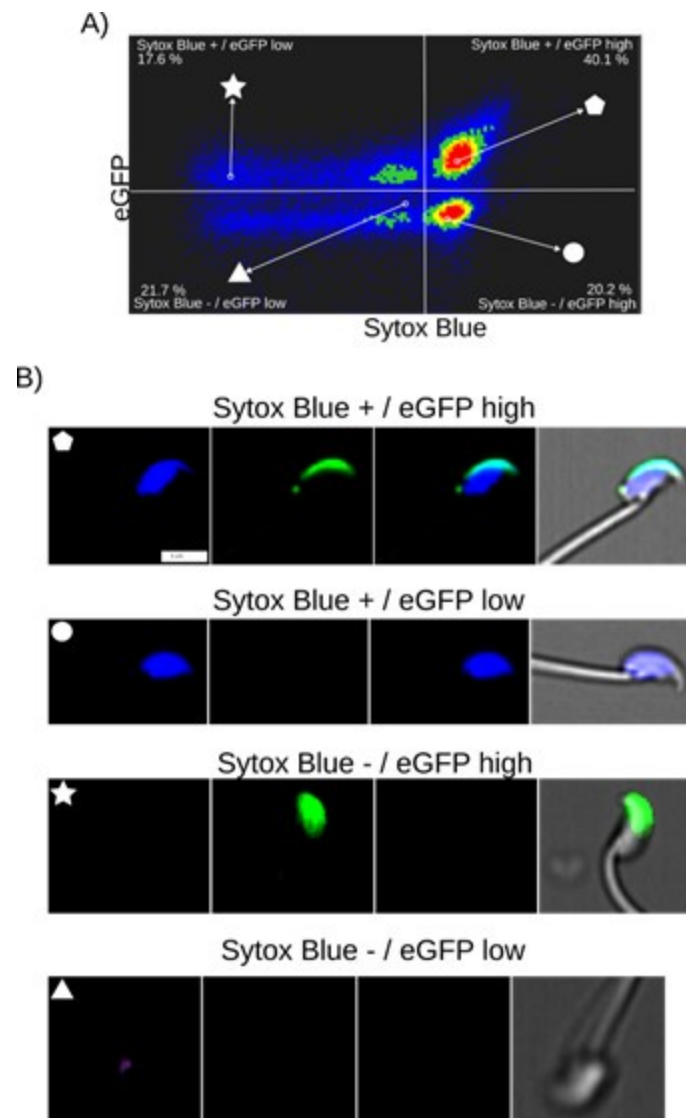
Author response image 1 illustrates the relationship between cell death and spontaneous AE in noncapacitated mouse sperm, where intact acrosomes are marked by EGFP. Cell death was evaluated using Sytox Blue staining, a dye that is impermeable to live cells and shows affinity for DNA. AE was assessed by the absence of EGFP in the acrosome.

Author response image 1a indicates a lack of correlation between Sytox and EGFP fluorescence. Two populations of sperm with EGFP signals were found (EGFP<sup>+</sup> and EGFP<sup>-</sup>), each showing a broad distribution of Sytox signal, enabling the distinction between cells that retain plasma membrane integrity (live sperm: Sytox<sup>-</sup>) and those with compromised membranes (dead cells: Sytox<sup>+</sup>). The observed bimodal distribution of EGFP signal, regardless of live versus dead cell populations, indicates that the fenestration of the plasma membrane known to occur during AE is a regulated process that does not necessarily compromise the overall plasma membrane integrity.

These observations are reinforced by the single-cell examples in Author response image 1b, where we were able to identify sperm in four categories: live sperm with intact acrosome (EGFP<sup>+</sup>/Sytox<sup>-</sup>), live sperm with acrosomal exocytosis (EGFP<sup>-</sup>/Sytox<sup>-</sup>), dead sperm with intact acrosome (EGFP<sup>+</sup>/Sytox<sup>+</sup>), and dead sperm with AE (EGFP<sup>-</sup>/Sytox<sup>+</sup>). Note the case of AE (lacking EGFP signal) which bears an intact plasma membrane (lacking Sytox Blue signal). Author response image 2 shows single-cell examples of the four categories observed with confocal microscopy to reinforce the observations from Author response image 1a.

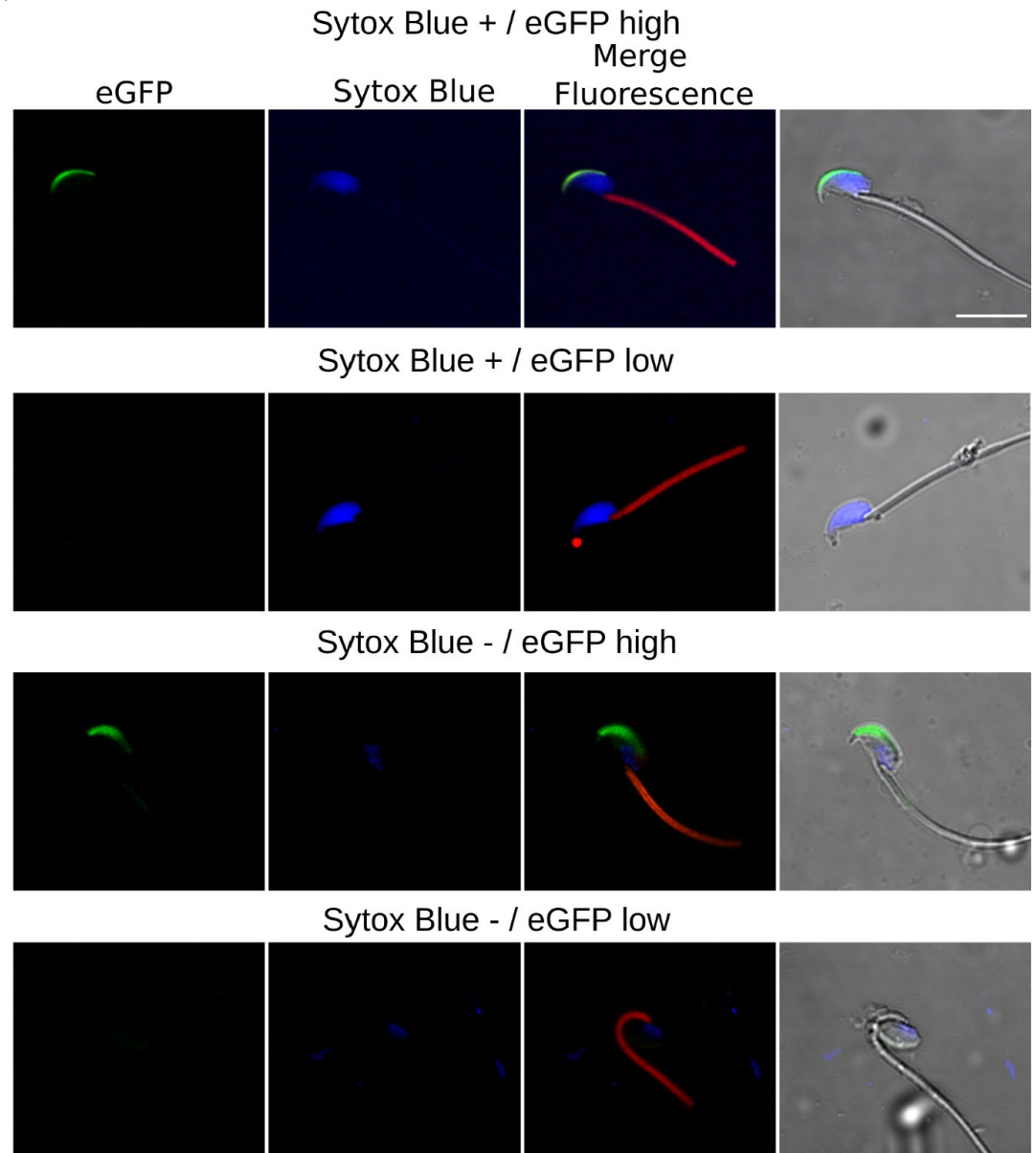
#### Author response image 1:

Fi. Image based flow cytometry analysis (ImageStream Merk II), of non-capacitated mouse sperm, showing the distribution of EGFP signal (acrosome integrity) against Sytox Blue staining (cell viability). **(A)** The quadrants show: Sytox Blue + / EGFP low (17.6%), Sytox Blue + / EGFP high (40.1%), Sytox Blue - / EGFP high (20.2%), and Sytox Blue - / EGFP low (21.7%). Each quadrant indicates the percentage of the total sperm population exhibiting the corresponding staining pattern. Axes are presented in a log<sub>10</sub> scale of arbitrary units of fluorescence. **(B)** Representative single-cell images corresponding to the four categorized sperm populations from the flow cytometry analysis in panel **(A)**. The top row displays sperm with compromised plasma membrane integrity (Sytox Blue +), showing low (left) and high (right) EGFP signals. The bottom row shows sperm with intact plasma membrane (Sytox Blue -), displaying high (left) and low (right) EGFP signal. It is worth noting that when analyzing the percentages in **(A)**, we observed that the data also encompass a population of headless flagella, which was present in all observed categories. Therefore, the percentages should be interpreted with caution.



#### Author response image 2:

Confocal Microscopy Examples of AE and cell viability. The top row features sperm with compromised plasma membrane integrity (Sytox Blue +) and high EGFP expression; the second row displays sperm with compromised membrane and low EGFP expression; the third row illustrates sperm with intact membrane (Sytox Blue -) and high EGFP expression; the bottom row shows sperm with intact membrane and low EGFP expression.



Author response images 3-5 provide insight into the relationship between FM4-64 and Sytox Blue fluorescence intensities in non-capacitated sperm (CTRL, Author response image 3), capacitated sperm and acrosome exocytosis events stimulated with 100  $\mu$ M progesterone (PG, Author response image 4), and capacitated sperm stimulated with 20  $\mu$ M ionomycin (IONO, Author response image 5). Two populations of sperm with Sytox Blue signals were clearly distinguished (Sytox+ and Sytox-), enabling the discernment between live and dead sperm. Interestingly, the upper right panels of Author response images 3A, 4A, and 5A (Sytox Blue+ / FM4-64 high) consistently show a positive correlation between FM4-64 and Sytox Blue. This observation aligns with the concern raised by Reviewer 2, suggesting that compromised membranes due to cell death provide more binding sites for FM4-64.

Nonetheless, the lower panels of Author response images 3A, 4A and 5A (Sytox Blue-) show no correlation with FM4-64 fluorescence, indicating that this population can exhibit either low or high FM4-64 fluorescence. As expected, in stark contrast with the CTRL case, the stimulation of AE with PG or IONO in capacitated sperm increased the population of live

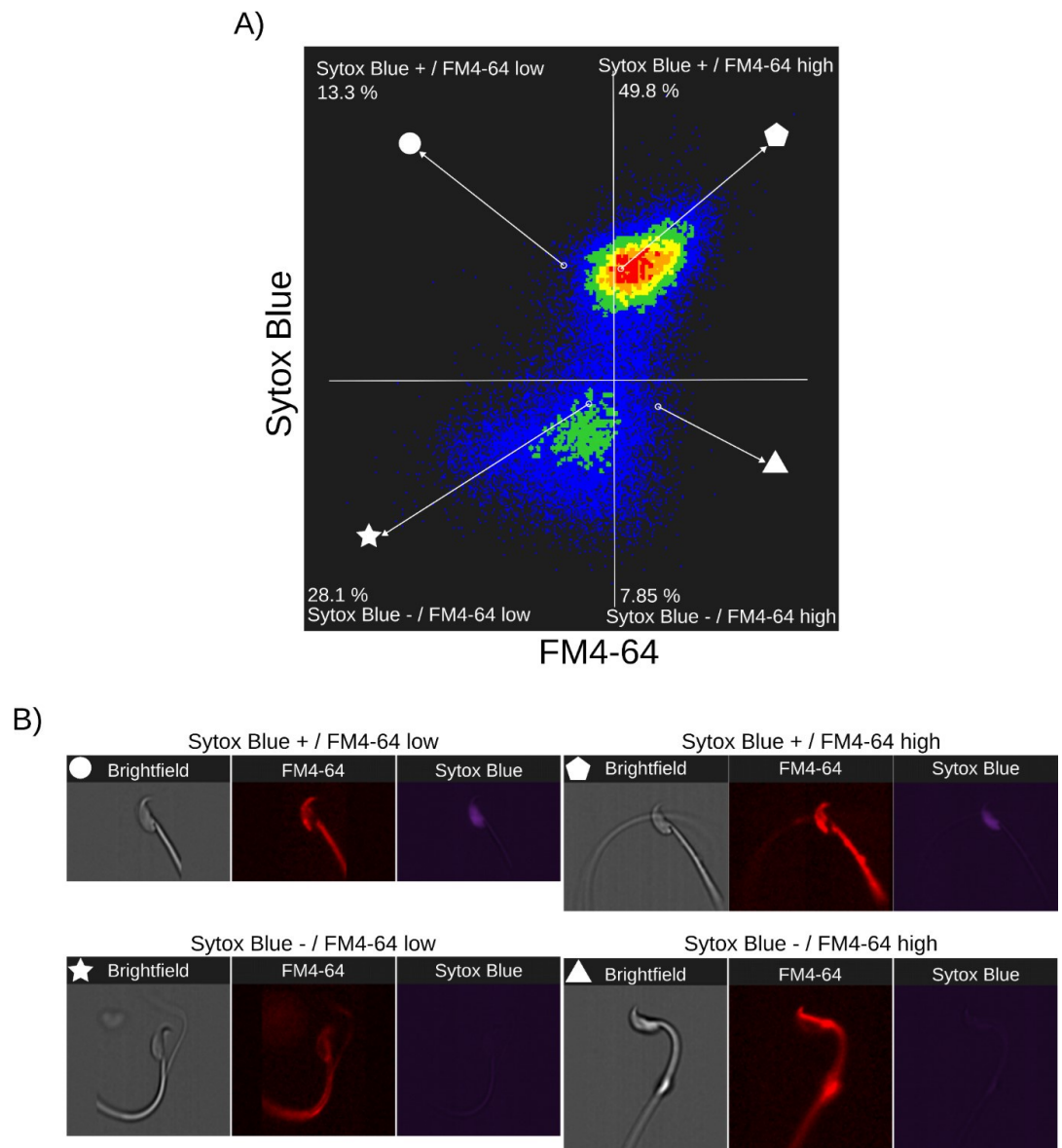


sperm with high FM4-64 fluorescence (Sytox Blue+ / FM4-64 high: CTRL: 7.85%, PG: 8.73%, IONO: 13.5%).

Single-cell examples are shown in Author response images 3B, 4B, and 5B, where the four categories are represented: dead sperm with low FM4-64 fluorescence (Sytox Blue+ / FM4-64 low), dead sperm with high FM4-64 fluorescence (Sytox Blue+ / FM4-64 high), live sperm with low FM4-64 fluorescence (Sytox Blue- / FM4-64 low), and live sperm with high FM4-64 fluorescence (Sytox Blue- / FM4-64 high).

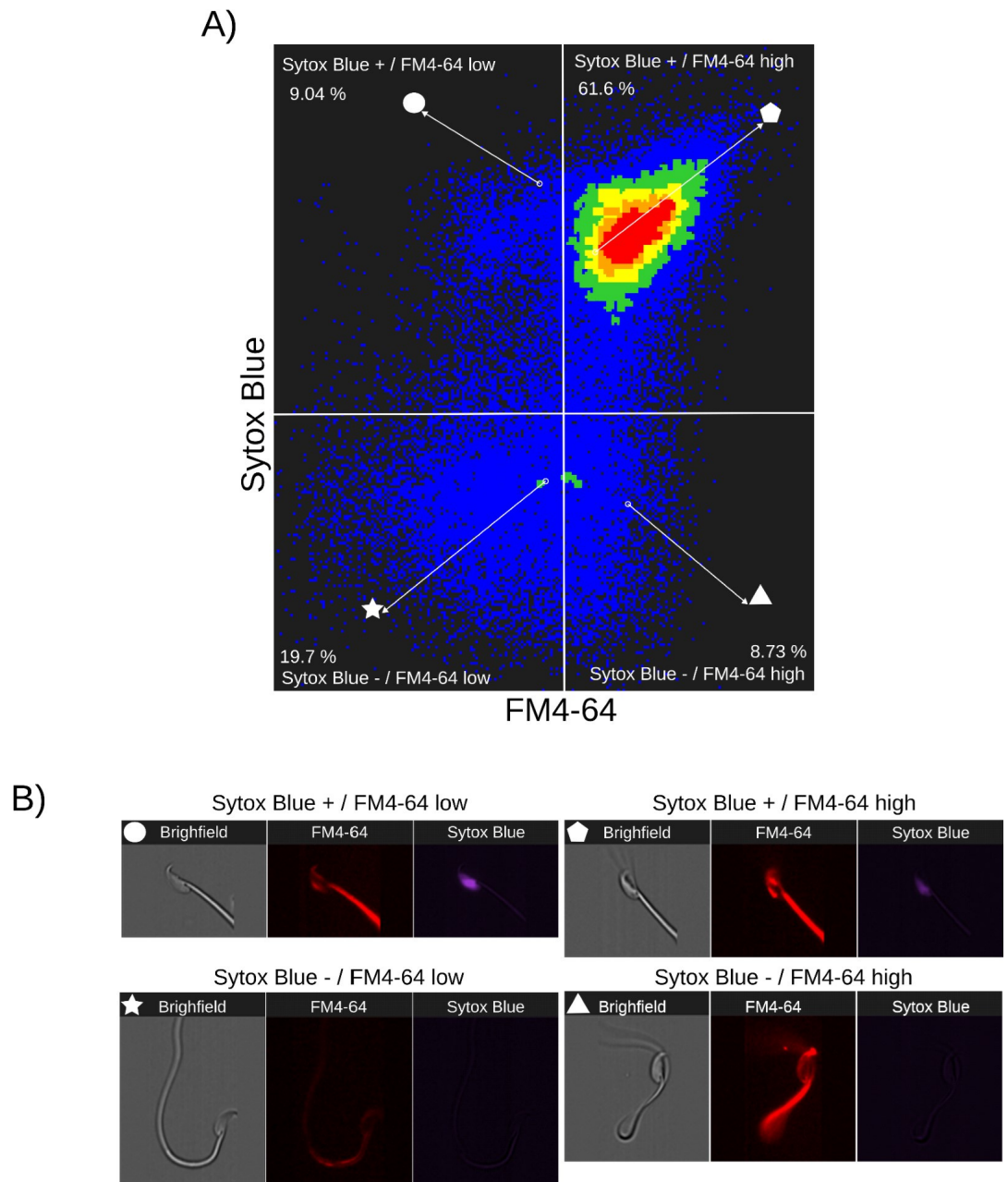
### Author response image 3:

Relationship between cell death and FM4-64 fluorescence in capacitated sperm without inductor of RA. Image-based flow cytometry analysis of non-capacitated mouse sperm loaded with FM464 and Sytox Blue dyes, with one and two minutes of incubation time, respectively. **(A)** The quadrants show: Sytox Blue+ / FM4-64 low (13.3%), Sytox Blue+ / FM4-64 high (49.8%), Sytox Blue- / FM4-64 low (28.1%), and Sytox Blue- / FM4-64 high (7.85%). Each quadrant indicates the percentage of the total sperm population exhibiting the corresponding staining pattern. Axes are presented on a log<sub>10</sub> scale of arbitrary units of fluorescence. **(B)** Representative single-cell images corresponding to the four categorized sperm populations from the flow cytometry analysis in panel (A).



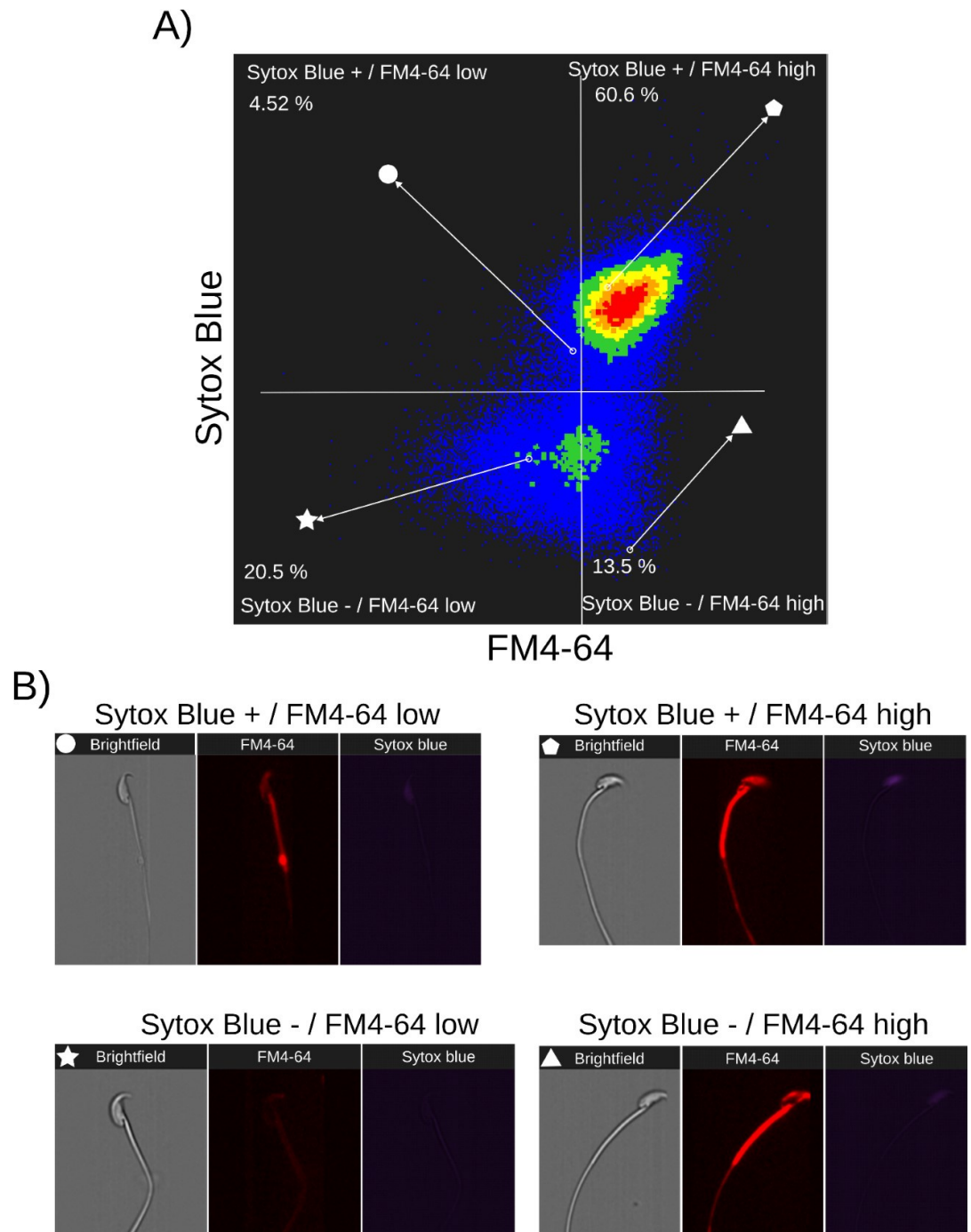
#### Author response image 4:

Relationship between cell death and FM4-64 fluorescence capacitated sperm stimulated with progesterone. Image-based flow cytometry analysis of non-capacitated mouse sperm loaded with FM4-64 and Sytox Blue dyes, with one and two minutes of incubation time, respectively. **(A)** The quadrants show: Sytox Blue+ / FM4-64 low (9.04%), Sytox Blue+ / FM4-64 high (61.6%), Sytox Blue- / FM4-64 low (19.7%), and Sytox Blue- / FM4-64 high (8.73%). Each quadrant indicates the percentage of the total sperm population exhibiting the corresponding staining pattern. Axes are presented on a log10 scale of arbitrary units of fluorescence. **(B)** Representative single-cell images corresponding to the four categorized sperm populations from the flow cytometry analysis in panel (A)



**Author response image 5:**

Relationship between cell death and FM4-64 fluorescence capacitated sperm stimulated with ionomycin. Image-based flow cytometry analysis of non-capacitated mouse sperm loaded with FM464 and Sytox Blue dyes, with one and two minutes of incubation time, respectively. **(A)** The quadrants show: Sytox Blue+ / FM4-64 low (4.52%), Sytox Blue+ / FM4-64 high (60.6%), Sytox Blue- / FM4-64 low (20.5%), and Sytox Blue- / FM4-64 high (13.5%). Each quadrant indicates the percentage of the total sperm population exhibiting the corresponding staining pattern. Axes are presented on a log10 scale of arbitrary units of fluorescence. **(B)** Representative single-cell images corresponding to the four categorized sperm populations from the flow cytometry analysis in panel (A).



Based on the data presented in Author response images 1 to 6, we derive the following conclusions summarized below:

- (1) There is no direct relationship between cell death (Sytox Blue-) and AE (EGFP) (Author response images 1 and 2).
- (2) There is bistability in the FM4-64 fluorescent intensity. Before reaching a certain threshold, there is no correlation between FM4-64 and Sytox Blue signals, indicating no cell death. However, after crossing this threshold, the FM4-64 signal becomes correlated with Sytox Blue+ cells, indicating cell death (Author response images 4-6).

(3) The Sytox Blue- population of capacitated sperm is sensitive to AE stimulation with progesterone, leading to the expected increase in FM4-64 fluorescence.

Therefore, while the FM4-64 signal alone is not a definitive marker for either AE or cell death, it is crucial to use additional viability assessments, such as Sytox Blue, to accurately differentiate between live and dead sperm in studies of acrosome exocytosis and sperm motility. In the present work, we did not use a cell viability marker due to the complex multicolor, multidimensional fluorescence experiments. However, cell viability was always considered, as any imaged sperm was chosen based on motility, indicated by a beating flagellum. The determination of whether selected sperm die during or after AE remains to be elucidated. The results presented in Figure 2 and Supplementary S1 show examples of motile sperm that experience an increase in FM4-64 fluorescence.

All this information is added to the manuscript (Supplementary Figure 1D).

*(4) It is unclear how the structural change in the midpiece causes the entire sperm flagellum, including the principal piece, to stop moving. It will be easier for readers to understand if the authors discuss possible mechanisms.*

Response P2.4: As requested, we have incorporated a possible explanation in the discussion section (see line 644-656). We propose three possible hypotheses for the cessation of sperm motility, which can be attributed to the simultaneous occurrence of various events:

- (1) Rapid increase in  $[Ca^{2+}]_i$  levels: A rapid increase in  $[Ca^{2+}]_i$  levels may trigger the activation of  $Ca^{2+}$  pumps within the flagellum. This process consumes local ATP levels, disrupting glycolysis and thereby depleting the energy required for motility.
- (2) Reorganization of the actin cytoskeleton: Alterations in the actin cytoskeleton can lead to changes in the mechanical properties of the flagellum, impacting its ability to move effectively.
- (3) Midpiece contraction: Contraction in the midpiece region can potentially interfere with mitochondrial function, impeding the energy production necessary for sustained motility.

*(5) The mitochondrial sheath and cell membrane are very close together when observed by transmission electron microscopy. The image in Figure 9A with the large space between the plasma membrane and mitochondria is misleading and should be corrected. The authors state that the distance between the plasma membrane and mitochondria approaches about 100 nm after the acrosome reaction (Line 330 - Line 333), but this is a very long distance and large structural changes may occur in the midpiece. Was there any change in the mitochondria themselves when they were observed with the DsRed2 signal?*

Response P2.5: The authors appreciate the reviewer's observation regarding the need to correct the image in Figure 9A, as the original depiction conveys a misleading representation of the spatial relationship between the mitochondrial sheath and the plasma membrane. This figure has been corrected to accurately reflect a more realistic proximity, while keeping in mind that it is a cartoonish representation.

Regarding the comments about the distances mentioned between former lines 330 and 333, the measurement was not intended to describe the gap between the plasma membrane and the mitochondria but rather the distance between F-actin and the plasma membrane.

Author response image 6 shows high-resolution scanning electron microscopy (SEM) of two sperm fixed with a protocol tailored to preserve plasma membranes (ref), where the insets clearly show the flagellate architecture in the midpiece with an intact plasma membrane



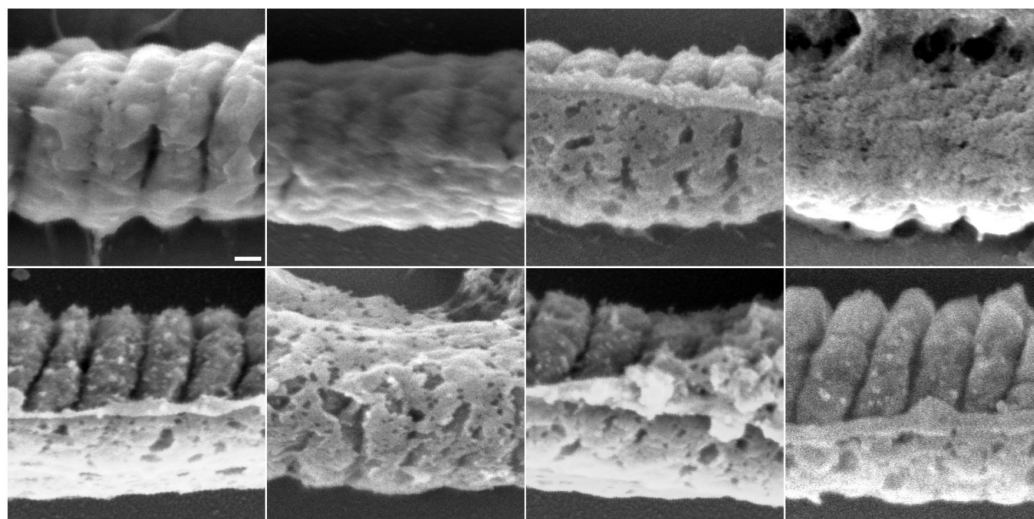
covering the mitochondrial network. A non-capacitated sperm with an intact acrosome is shown in panel A, and a capacitated sperm that has experienced AE is shown in panel B.

Notably, the results depicted in Author response image 6 demonstrate that, irrespective of the AE status, the distance between the plasma membrane and mitochondria consistently remains less than 20 nm, thus confirming the close proximity of these structures in both physiological states. As Reviewer 2 pointed out, if there is no significant difference in the distance between the plasma membrane and mitochondria, then the observed structural changes in the actin network within the midpiece should somehow alter the actual deposition of mitochondria within the midpiece. Figure 5D-F shows that midpiece contraction is associated with a decrease in the helical pitch of the actin network; the distance between turns of the actin helix decreases from  $l = 248$  nm to  $l = 159$  nm. This implies a net change in the number of turns the helix makes per 1  $\mu\text{m}$ , from 4 to 6  $\mu\text{m}^{-1}$ .

#### Author response image 6.

SEM image showing the proximity between plasma membrane and mitochondria. Scale bar 100 nm.

A)

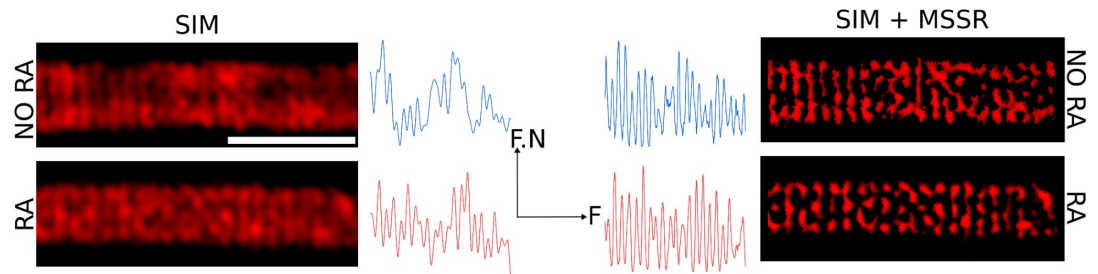


Additionally, a structural contraction can be observed in Figure 5D-F, where the radius of the helix decreases by about 50 nm. To clarify this point, we sought to measure the deposition of individual DsRed2 mitochondria using computational superresolution microscopy—FF-SRM (SRRF and MSSR), Structured Illumination Microscopy (SIM), or a combination of both (SIM + MSSR), in 2D. Author response image 7 shows that these three approaches allow the observation of individual DsRed mitochondria; however, the complexity of their 3D arrangement, combined with the limited space between mitochondria (as seen in Author response image 6), precludes a reliable estimation of mitochondrial organization within the midpiece. To overcome these challenges, we decided to study the midpiece architecture via SEM experiments on non-capacitated versus capacitated sperm stimulated with ionomycin to undergo the AE.

#### Author response image 7.

Organization of mitochondria observed via FF-SRM and SIM. Scale bar 2  $\mu\text{m}$ . F.N: Fluorescence normalized. F: Frequency

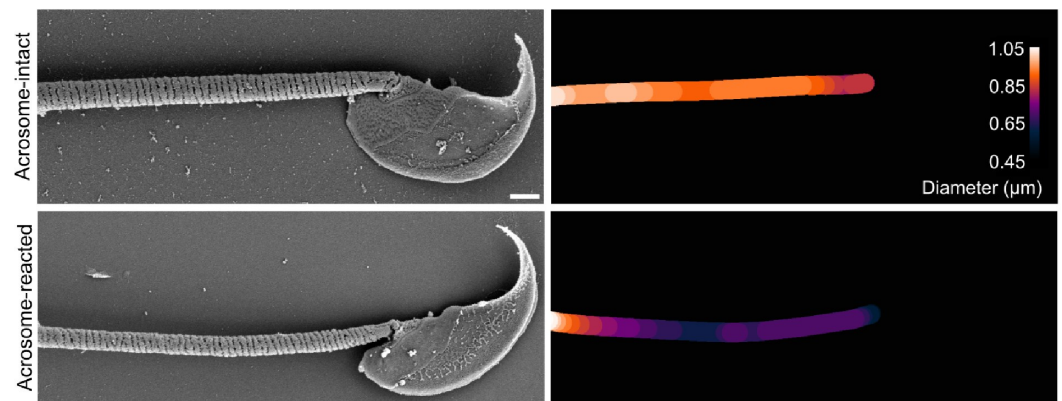




Author response image 8 presents a single-cell comparison of the midpiece architecture in noncapacitated (NC) and acrosome-intact (AI) versus acrosome-reacted (AR) sperm, along with measurements of the midpiece diameter throughout its length. Notably, the diameter of the midpiece increases from the base of the head to more distal regions, ranging from 0.45 nm to 1.10  $\mu\text{m}$  (as shown in Author response images 7 and 8). A significant correlation between the diameter of the flagellum and its curvature was observed (Author response image 9), suggesting a reorganization of the midpiece due to shearing forces. This is further exemplified in Author response images 8 and 9, which provide individual examples of this phenomenon.

#### Author response image 8.

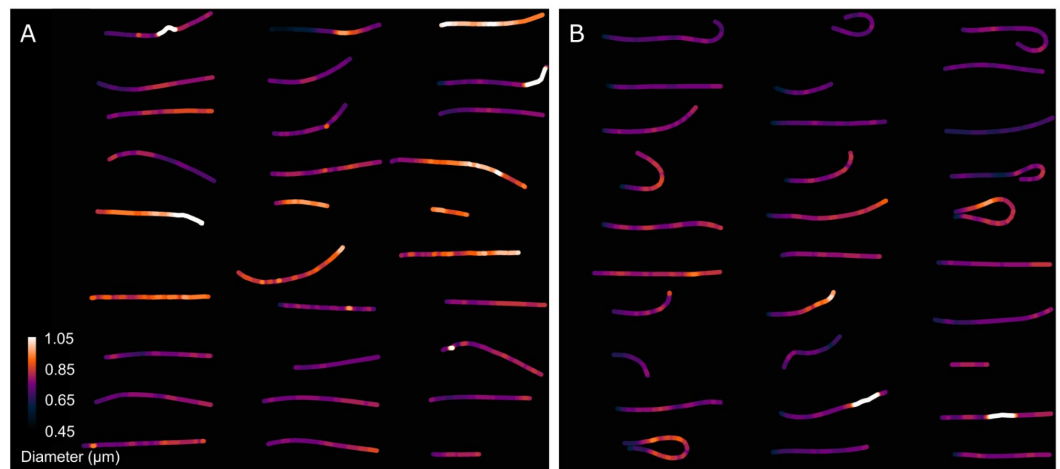
Comparison of the midpiece architecture in acrosome-intact and acrosome-reacted sperm using scanning electron microscopy (SEM).



As expected, the overall diameter of the midpiece in AI sperm was larger than in AR sperm, with measurements of  $0.731 \pm 0.008 \mu\text{m}$  for AI and  $0.694 \pm 0.007 \mu\text{m}$  for AR ( $p = 0.013$ , Kruskal-Wallis test  $n > 100$ ,  $N = 2$ ), as shown in Author response image 10. Additionally, this Author response image 7 indicates that the reorganization of the midpiece architecture involves a change in the periodicity of the mitochondrial network, with frequencies shifting from  $f_{\text{NC}}$  to  $f_{\text{EA}}$  mitochondria per micron.

#### Author response image 9.

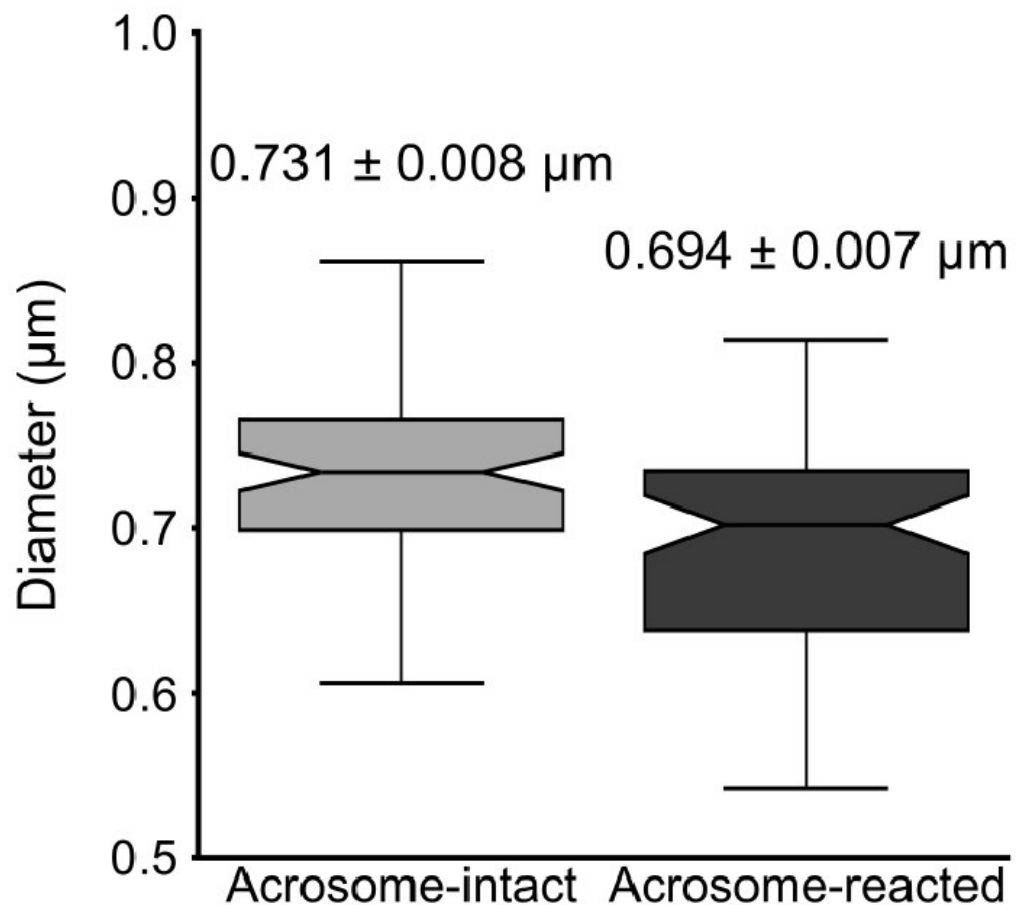
Comparison of the midpiece architecture in acrosome-intact (A) and acrosome-reacted (B) sperm using scanning electron microscopy (SEM).



Collectively, the structural results presented in Figure 5 and Author response images 6 to 10 demonstrate that the AE involves a comprehensive reorganization of the midpiece, affecting its diameter, pitch, and the organization of both the actin and mitochondrial networks. All this information is now incorporated in the new version of the paper (Figure. 2F)

#### Author response image 10.

Quantification of the midpiece diameter of the sperm flagellum in acrosome-intact and acrosome-reacted sperm analyzed by scanning electron microscopy (SEM). Data is presented as mean  $\pm$  SEM. Kruskal-Wallis test was employed,  $p = 0.013$  (AI  $n=85$  , AR  $n=72$ ).



(6) In the TG sperm used, the green fluorescence of the acrosome disappears when sperm die. Figure 1C should be analyzed only with live sperm by checking viability with propidium iodide or other means.

Response P2.6: We concur with Reviewer 2 that ideally, any experiment conducted for this study should include an intrinsic cell viability test. However, the current research employs a wide array of multidimensional imaging techniques that are not always compatible with, or might be suboptimal for, simultaneous viability assessments. In agreement with the reviewer's concerns, it is recognized that the data presented in Figure 1C may inherently be biased due to cell death. Nonetheless, Author response image 1 demonstrates that the relationship between AE and cell death is more complex than a straightforward all-or-nothing scenario. Specifically, Author response image 1C illustrates a case where the plasma membrane is compromised (Sytox Blue+) yet maintains acrosomal integrity (EGFP+). This observation contradicts Reviewer 1's assertion that "the green fluorescence of the acrosome disappears when sperm die," as discussed more comprehensively in response P2.3.

In light of these observations, we have meticulously revisited the entire manuscript to address and clarify potential biases in our results due to cell death. Consequently, Author response image 5 and its detailed description have been incorporated into the supplementary material of the manuscript to contribute to the transparency and reliability of our findings.

### Reviewer #3 (Public Review):

*(1) While progressive and also hyperactivated motility are required for sperm to reach the site of fertilization and to penetrate the oocyte's outer vestments, during fusion with the oocyte's plasma membrane it has been observed that sperm motility ceases. Identifying the underlying molecular mechanisms would provide novel insights into a crucial but mostly overlooked physiological change during the sperm's life cycle. In this publication, the authors aim to provide evidence that the helical actin structure surrounding the sperm mitochondria in the midpiece plays a role in regulating sperm motility, specifically the motility arrest during sperm fusion but also during earlier cessation of motility in a subpopulation of sperm post acrosomal exocytosis. The main observation the authors make is that in a subpopulation of sperm undergoing acrosomal exocytosis and sperm that fuse with the plasma membrane of the oocyte display a decrease in midpiece parameter due to a 200 nm shift of the plasma membrane towards the actin helix. The authors show the decrease in midpiece diameter via various microscopy techniques all based on membrane dyes, bright-field images and other orthogonal approaches like electron microscopy would confirm those observations if true but are missing. The lack of additional experimental evidence and the fact that the authors simultaneously observe an increase in membrane dye fluorescence suggests that the membrane dyes instead might be internalized and are now staining intracellular membranes, creating a false-positive result. The authors also propose that the midpiece diameter decrease is driven by changes in sperm intracellular  $Ca^{2+}$  and structural changes of the actin helix network. Important controls and additional experiments are needed to prove that the events observed by the authors are causally dependent and not simply a result of sperm cells dying.*

Response P3.1: We appreciate the reviewer's observations and critiques. In response, we have expanded our experimental approach to include alternative methodologies such as mathematical modeling and electron microscopy, alongside further fluorescence microscopy studies. This diversified approach aims to mitigate potential interpretation artifacts and substantiate the validity of our observations regarding the contraction of the sperm midpiece. Additionally, we have implemented further control experiments to fortify the credibility and robustness of our findings, ensuring a more comprehensive and reliable set of results.

First, we acknowledge the concerns raised by Reviewer 2 regarding the interpretation of the magnitude of the observed contraction of the sperm flagellum's midpiece (see response P2.5). Specifically, we believe that the assertion that "... there is a decrease in midpiece parameter due to a 200 nm shift of the plasma membrane towards the actin helix" stated by reviewer 3 needs careful examination. We recognize that the fluorescence microscopy data provided might not conclusively support such a substantial shift. Our live cell imaging and superresolution microscopy experiments indicate that there is a significant decrease in the diameter of the sperm flagellum associated with AE. This is supported by colocalization experiments where FM4-64-stained structures (fluorescing upon binding to membranes) are observed moving closer to Sir-Actinlabeled structures (binding to F-actin). Quantitatively, Figure S5 describes the spatial shift between FM4-64 and Sir-Actin signals, narrowing from a range of 140-210 nm to 50-110 nm (considering the 2nd and 3rd quartiles of the distributions). The mean separation distance between both signals changes from 180 nm in AI cells to 70 nm in AR cells, a net shift of 110 nm. This observation suggests caution regarding the claim of a "200 nm shift of the plasma membrane towards the actin cortex."

Moreover, the concerns raised by Reviewer #3 about the potential internalization of membrane dyes, which might create a false-positive result by staining intracellular membranes, offer an alternative mechanism to explain a shift of up to 100 nm. This perspective is also supported by the critique from Reviewer #2 regarding the substantial

distance (about 100 nm) between the plasma membrane and mitochondria post-acrosome reaction: “The authors state that the distance between the plasma membrane and mitochondria approaches about 100 nm after the acrosome reaction (...), but this is a very long distance and large structural changes may occur in the midpiece”. These insights have prompted us to refine our methodology and interpretation of the data to ensure a more accurate representation of the underlying biological processes.

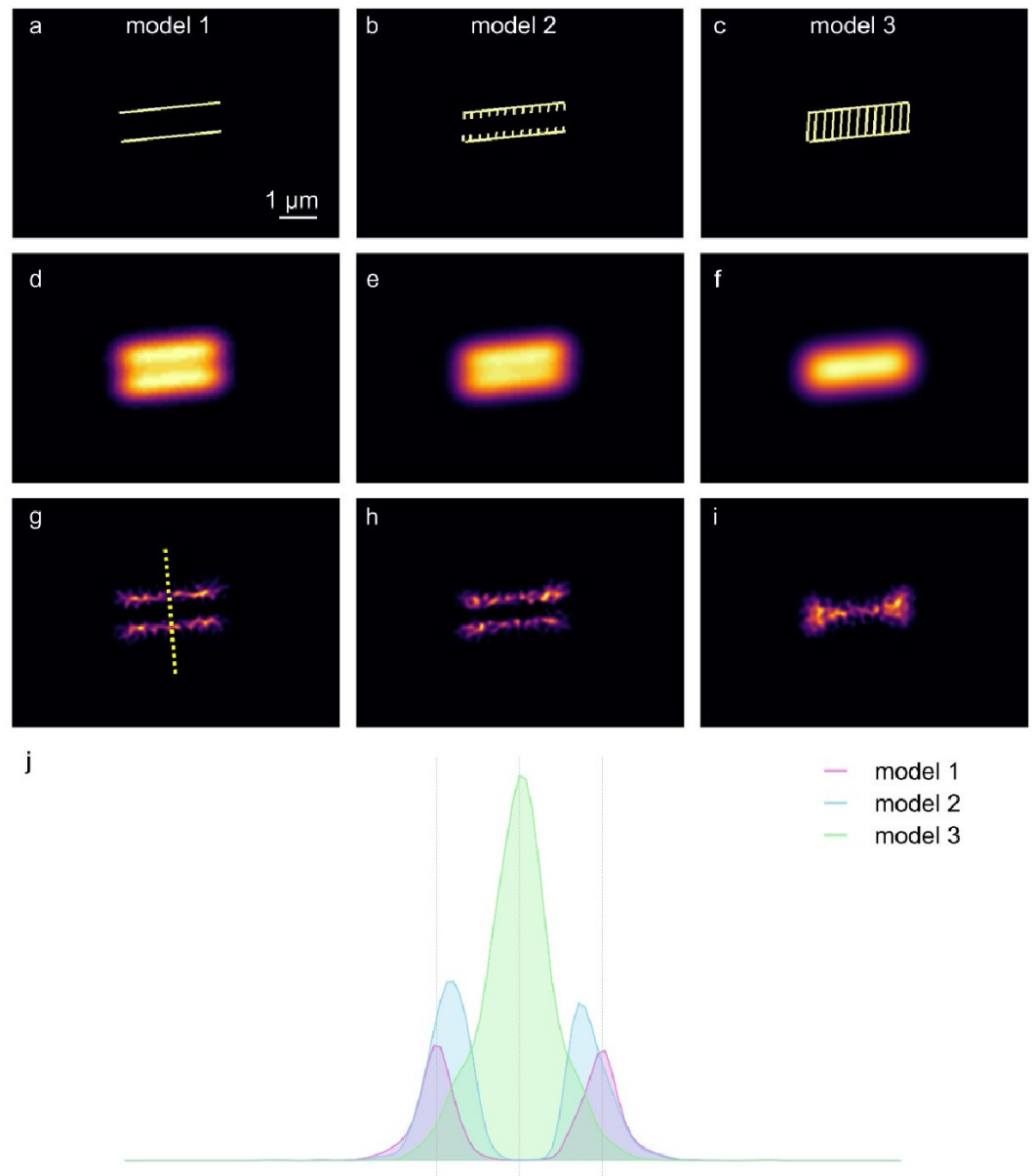
Author response image 11 shows a first principles approach in two spatial dimensions to explore three scenarios where a membrane dye, such as FM4-64, stains structures at and within the midpiece of a sperm flagellum, but yet does not result in a net change of diameter. Author response image 11A-C illustrates three theoretical arrangements of fluorescent dyes: Model 1 features two rigid, parallel structures that mimic the plasma membrane surrounding the midpiece of the flagellum. Model 2 builds on Model 1 by incorporating the possibility of dye internalization into structures located near the membrane, suggesting a slightly more complex interaction with nearby membranous intracellular structures. Model 3 represents an extreme scenario where the fluorescent dyes stain both the plasma membrane and internal structures, such as mitochondrial membranes, indicating extensive dye penetration and binding. Author response image 11D-F displays the convolution of the theoretical fluorescent signals from Models 1 to 3 with the theoretical point spread function (PSF) of a fluorescent microscope, represented by a Gaussian-like PSF with a sigma of 19 pixels (approximately 300 nm). This process simulates how each model's fluorescence would manifest under microscopic observation, showing subtle differences in the spatial distribution of fluorescence among the models. Author response image 11G-I reveals the superresolution images obtained through Mean Shift Super Resolution (MSSR) processing of the models depicted in Author response image 11D-F.

By analyzing the three scenarios, it becomes clear that the signals from Models 2 and 3 shift towards the center compared to Model 1, as depicted in Author response image 11J. This shift in fluorescence suggests that the internalization of the dye and its interaction with internal structures might significantly influence the perceived spatial distribution and intensity of fluorescence, thereby impacting the interpretation of structural changes within the midpiece. Consequently, the experimentally observed contraction of up to 100 nm in could represent an actual contraction of the sperm flagellum's midpiece, a relocalization of the FM4-64 membrane dyes to internal structures, or a combination of both scenarios.

To discern between these possibilities, we implemented a scanning electron microscopy (SEM) approach. The findings presented in Figure 5 and Author response images 7 to 9 conclusively demonstrate that the AE involves a comprehensive reorganization of the midpiece. This reorganization affects its diameter, which changes by approximately 50 nm, as well as the pitch and the organization of both the actin and mitochondrial networks. This data corroborates the structural alterations observed and supports the validity of our interpretations regarding midpiece dynamics during the AE.

### **Author response image 11**

Modeling three scenarios of midpiece staining with membrane fluorescent dyes.



Secondly, we wish to clarify that in some of our experiments, we have utilized changes in the intensity of FM4-64 fluorescence as an indirect measure of midpiece contraction. This approach is supported by a linear inverse correlation between these variables, as illustrated in Figure S2D. It is important to note that this observation is correlative and indirect; therefore, our data does not directly substantiate the claim that "in a subpopulation of sperm undergoing AE and sperm that fuse with the plasma membrane of the oocyte, there is a decrease in midpiece parameter due to a 200 nm shift of the plasma membrane towards the actin helix". Specifically, we have not directly measured the distance between the plasma membrane and actin cortex in experiments involving gamete fusion.

All the concerns highlighted in this Response P1.1 have been addressed and incorporated into the manuscript. This addition aims to provide comprehensive insight into the experimental observations and methodologies used, ensuring that the data is transparent and accessible for thorough review and replication.



### **Editor Comment:**

*As the authors can see from the reviews, the reviewers had quite different degrees of enthusiasm, thus discussed extensively. The major points in consensus are summarized below and it is highly recommended that the authors consider their revisions.*

*(1) Causality of midpiece contraction with motility arrest is not conclusively supported by the current evidence. Time-resolved imaging of FM4-64 and motility is needed and the working model needs to be revised with two scenarios - whether the sperm contracting indicates a fertilizing sperm or sperm to be degenerated.*

*(2) The rationale for using FM4-64 as a plasma membrane marker is not clear as it is typically used as an endo-membrane marker, which is also related to the discrepancy of Fluo-4 signal diameter vs. FM4-64 (Figure 4E). The viability of sperm with increased FM4-64 needs to be demonstrated.*

*(3) The mechanism of midpiece contraction in motility cessation along the whole flagellum is not discussed.*

*(4) The use of an independent method to support the changes in midpiece diameter/structural changes such as DsRed (transgenic) or TEM.*

*(5) The claim of  $Ca^{2+}$  change needs to be toned down.*

Response Editor: We thank the editor and the reviewers for their thorough and positive assessment of our work and the constructive feedback to further improve our manuscript. Please find below our responses to the reviewers' comments. We have addressed all these points in the current version. Briefly,

(1) Time resolved images to show the correlation between FM4-64 fluorescence increase and the motility was incorporated

(2) The rationale for using FM4-64 was added.

(3) The mechanism of midpiece contraction was discussed in the paper

(4) An independent method was included to support our conclusions (SEM and other markers not based on membrane dyes)

(5) The results related to the calcium increase were toned down.

### **Recommendations for the authors:**

#### **Reviewer #1 (Recommendations For The Authors):**

*(1) To claim midpiece actin polymerization/re-organization is required for AE, demonstrating that AE does not occur in the presence of actin depolymerizing drugs (e.g., Latrunculin A, Cytochalasin D) would be necessary since the current data only shows the association/correlation. Was the block of AE by actin depolymerization observed?*

Response R1.1: We agree with the reviewer but unfortunately, since actin polymerization and or depolymerization in the head are important for exocytosis, we cannot use this experimental approach to dissect both events. Addition of these inhibitors block the occurrence of AE (PMID: 12604633).

*(2) Please provide the rationale for using FM4-64 to visualize the plasma membrane since it has been reported to selectively stain membranes of vacuolar organelles. What is the principle of increase of FM4-64 dye intensity, other than the correlation with midpiece contraction? For example, in lines 400-402: the authors mentioned that 'some acrosomereacted moving sperm within the perivitelline space had low FM4-64 fluorescence in the midpiece (Figure 6C). After 20 minutes, these sperm stopped moving and exhibited increased FM4-64 fluorescence, indicating midpiece contraction (Figure 6D).' While recognizing the increase of FM4-64 dye intensity can be an indicator of midpiece contraction, without knowing how and when the intensity of FM4-64 dye changes, it is hard to understand this observation. Please discuss.*

Response R1.2: FM4-64 is an amphiphilic styryl fluorescent dye that preferentially binds to the phospholipid components of cell membranes, embedding itself in the lipid bilayer where it interacts with phospholipid head groups. Due to its amphiphilic nature, FM dyes primarily anchor to the outer leaflet of the bilayer, which restricts their internalization. It has been demonstrated that FM4-64 enters cells through endocytic pathways, making these dyes valuable tools for studying endocytosis.

Upon binding, FM4-64's fluorescence intensifies in a more hydrophobic environment that restricts molecular rotation, thus reducing non-radiative energy loss and enhancing fluorescence. These photophysical properties render FM dyes useful for observing membrane fusion events. When present in the extracellular medium, FM dyes rapidly reach a chemical equilibrium and label the plasma membrane in proportion to the availability of binding sites.

In wound healing studies, for instance, the fluorescence of FM4-64 is known to increase at the wound site. This increase is attributed to the repair mechanisms that promote the fusion of intracellular membranes at the site of the wound, leading to a rise in FM4-64 fluorescence. Similarly, an increase in FM4-64 fluorescence has been reported in the heads of both human and mouse sperm, coinciding with AE. In this scenario, the fusion between the plasma membrane and the acrosomal vesicle provides additional binding sites for FM4-64, thus increasing the total fluorescence observed in the head. This dynamic response of FM4-64 makes it an excellent marker for studying these cellular processes in real-time.

This study is the first to report an increase in FM4-64 fluorescence in the midpiece of the sperm flagellum. Figures 5 and Author response images 6 to 9 demonstrate that during the contraction of the sperm flagellum, structural rearrangements occur, including the compaction of the mitochondrial sheath and other membranous structures. Such contraction likely increases the local density of membrane lipids, thereby elevating the local concentration of FM4-64 and enhancing the probability of fluorescence emission. Additionally, changes in the microenvironment such as pH or ionic strength during contraction might further influence FM4-64's fluorescence properties, as detailed by Smith et al. in the Journal of Membrane Biology (2010). The photophysical behavior of FM4-64, including changes in quantum yield due to tighter membrane packing or alterations in curvature or tension, may also contribute to the increased fluorescence observed. Notably, Figure S2 indicates that other fluorescent dyes like Memglow 700, Bodipy-GM, and FM1-43 also show a dramatic increase in their fluorescence during the midpiece contraction. Investigating whether the compaction of the plasma membrane or other mesoscale processes occur in the midpiece of the sperm flagellum could be a valuable area for future research. The use of fluorescent dyes such as LAURDAN or Nile Red might provide further insights into these membrane dynamics, offering a more comprehensive understanding of the biochemical and structural changes during sperm motility and gamete fusion events.

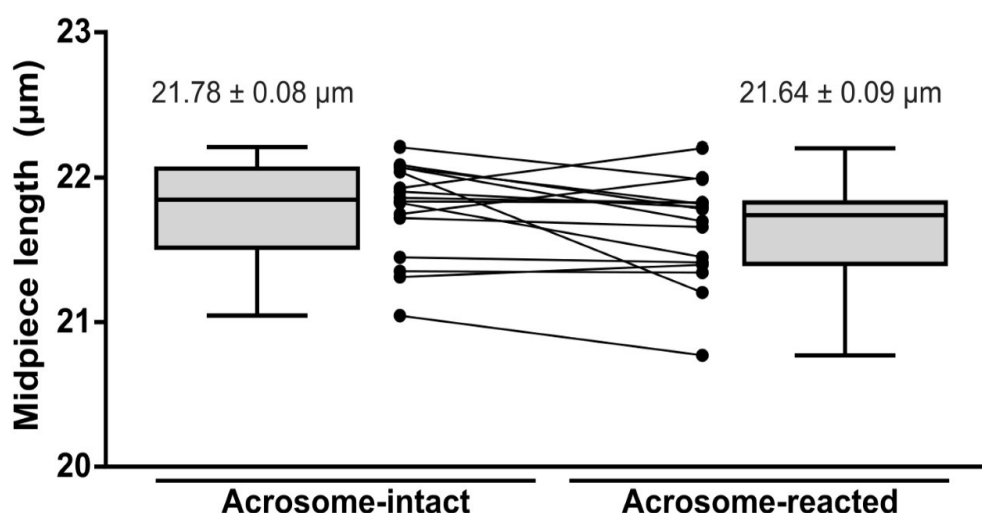
*(3) As the volume of the whole midpiece stays the same while the diameter decreases along the whole midpiece (midpiece contraction), the authors need to describe what*

*changes in the midpiece length they observe during the contraction. Was the length of the midpiece during the contraction measured and compared before and after contraction?*

Response R1.3: As requested, we have measured the length of the midpiece in AI and AR sperm. As shown in Author response image 12 (For review purposes only), no statistically significant differences were observed.

**Author response image 12.**

Midpiece length measured by the length of mitochondrial DsRed2 fluorescence in EGFP-DsRed2 sperm. Measurements were done before (acrosome-intact) and after (acrosome-reacted) acrosome exocytosis and midpiece contraction. Data is presented as the mean  $\pm$  sem of 14 cells induced by 10  $\mu$ M ionomycin. Paired t-test was performed, resulting in no statistical significance.



*(4) Most of all, it is not clear what the midpiece, thus mitochondria, contraction means in terms of sperm bioenergetics and motility cessation. Would the contraction induce mitochondrial depolarization or hyperpolarization, increase or decrease of ATP production/consumption? It will be great if this point is discussed. For example, an increase in mitochondrial Ca<sup>2+</sup> is a good indicator of mitochondrial activity (ATP production).*

Response R1.4: That is an excellent point. We have discussed this idea in the discussion (line 620-624). We are currently exploring this idea using different approaches because we also think that these changes in the midpiece may have an impact in the function of the mitochondria and perhaps, in their fate once they are incorporated in the egg after fertilization.

*(5) The authors claimed that Ca<sup>2+</sup> signal propagates from head to tail, which is the opposite of the previous study (PMID: 17554080). Please clarify if it is a speculation. Otherwise, please support this claim with direct experimental evidence (e.g., high-speed calcium imaging of single cells).*

Response R1.5: In that study, it was claimed that a  $[Ca^{2+}]_i$  increase that propagates from the tail to the head occurs when CatSper is stimulated. They did not evaluate the occurrence of AE when monitoring calcium.

Our data is in agreement with our previous results (PMID: 26819478) that consistently indicated that only the  $[Ca^{2+}]_i$  rise originating in the sperm head is able to promote AE.

*(6) Figure 4E: Please explain how come Fluo4 signal diameter can be smaller than FM4-64 dye if it stains plasma membrane (at 4' and 7').*

Response R1.6: When colocalizing a diffraction-limited image (Fluo4) with a super-resolution image (FM4-64), discrepancies in signal sizes and locations can become apparent due to differences in resolution. The Fluo4 signal, being diffraction-limited, adheres to a resolution limit of approximately 200-300 nanometers under conventional light microscopy. This limitation causes the fluorescence signal to appear broader and less defined. Conversely, super-resolution microscopy techniques, such as SRRE (Super-Resolution Radial Fluctuations), achieve resolutions down to tens of nanometers, allowing FM4-64 to reveal finer details at the plasma membrane and display potentially smaller apparent sizes of stained structures. Although both dyes might localize to the same cellular regions, the higher resolution of the FM4-64 image allows it to show a more precise and smaller diameter of the midpiece of the flagellum compared to the broader, less defined signal of Fluo4. To address this, the legend of Figure 4E has been slightly modified to clarify that the FM4-64 image possesses greater resolution.

*(7) Figure 5D-G: the midpiece diameter of AR intact cells was shown ~ 0.8  $\mu$ m or more in Figure 2, while now the radius in Figure 5 is only 300 nm. Since the diameter of the whole midpiece is nearly uniform when the acrosome is intact, clarify how and what brings this difference and where the diameter/radius measurement is done in each figure.*

Response R1.7: The difference resides in what is being measured. In Figure 2, the total diameter of the cell is measured, through the maximum peaks of FM4-64 fluorescence which is a probe against plasma membrane. As for Figure 5, the radius shown makes reference to the radius of the actin double helix within the midpiece. To that end, cells were fixed and stained with phalloidin, a F-actin probe.

*Minor points*

*(8) Figure S1 title needs to be changed. The "Midpiece contraction" concept is not introduced when Figure S1 is referred to.*

Response R1.8: This was corrected in the new version.

*(9) Reference #19: the authors are duplicated.*

Response R1.9: This was corrected in the new version.

*(10) Line 315-318: sperm undergoing contraction -> sperm undergoing AR/AE?*

Response R1.10: This was corrected in the new version.

*(11) Line 3632 -> punctuation missing.*

Response R1.11: Modified as requested.

(12) Movie S7: please add an arrow to indicate the spermatozoon of interest.

Response R1.12: The arrow was added as suggested.

(13) Line 515: *One result of this study was that the sperm flagellum folds back during fusion coincident with the decrease in the midpiece diameter. The authors did not provide an explanation for this observation. Please speculate the function of this folding for the fertilization process.*

Response R1.13: As requested, this is now incorporated in the discussion. We speculate that the folding of the flagellum during fusion further facilitates sperm immobilization because it makes it more difficult for the flagellum to beat. Such processes can enhance stability and increase the probability of fusion success. Mechanistically, the folding may occur as a consequence of the deformation-induced stress that develops during the decrease of midpiece diameter.

**Reviewer #2 (Recommendations For The Authors):**

(1) Figure 2C, D, E. Does "-1" on the X-axis mean one minute before induction? If so, the diameter is already smaller and FM4-64 fluorescence intensity is higher before the induction in the spontaneous group. Does the acrosome reaction already occur at "-1" in this group?

Response R2.1: Yes, "-1" means that the measurements of the diameter/FM4-64 fluorescence was done one minute before the induction. And it is correct that the diameter is smaller and FM464 fluorescence higher in the spontaneous group because these sperm underwent acrosome exocytosis before the induction, that is, spontaneously.

(2) Figure 3D. Purple dots are not shown in the graph on the right side.

Response R2.2: Modified as requested.

(3) Lines 404-406. *"These results suggest that midpiece contraction and motility cessation occur only after acrosome-reacted sperm penetrate the zona pellucida". Since midpiece contraction and motility cessation also occur before the passage through the zona pellucida (Figure 9B), "only" should be deleted.*

Response R2.3: Modified as requested.

**Reviewer #3 (Recommendations For The Authors):**

(1) *Do the authors have a hypothesis as to why the observed decrease in midpiece parameter results in cessation of sperm motility? It would be beneficial for the manuscript to include a paragraph about potential mechanisms in the discussion.*

Response R3.1: As requested, a potential mechanism has been proposed in the discussion section (line 644-656).

(2) *Since the authors propose in Gervasi et al. 2018 that the actin helix might be responsible for the integrity of the mitochondrial sheath and the localization of the mitochondria, is it possible that the proposed change in plasma membrane diameter and actin helix remodeling for example alters the localization of the mitochondria? TEM should be able to reveal any associated structural changes. In its current state, the manuscript lacks experimental evidence supporting the author's claim that the "helical*

*actin structure plays a role in the final stages of motility regulation". The authors should either include additional evidence supporting their hypothesis or tone down their conclusions in the introduction and discussion.*

Response R3.3: We agree with the reviewer. This is an excellent point. As suggested by this reviewer as well as the other reviewers, we have performed SEM to observe the changes in the midpiece observed after its contraction for two main reasons. First, to confirm this observation using a different approach that does not involve the use of membrane dyes. As shown in Author response image 6-10, we have observed that in addition to the midpiece diameter, there is a reorganization of the mitochondria sheet that is also suggested by the SIM experiments. These observations will be explored with more experiments to confirm the structural and functional changes that mitochondria undergo during the contraction. We are currently investigating this phenomenon, These results are now included in the new Figure 2F.

*(3) In line 134: The authors write: 'Some of the acrosome reacted sperm moved normally, whereas the majority remained immotile'. Do the authors mean that a proportion of the sperm was motile prior to acrosomal exocytosis and became immotile after, or were the sperm immotile to begin with? Please clarify.*

Response R3.4: This statement is based on the quantification of the motile sperm after induction of AE within the AR population (Fig. 1C).

*(4) The authors do not provide any experimental evidence supporting the first scenario. In video 1 a lot of sperm do not seem to be moving to begin with, only a few sperm show clear beating in and out of the focal plane. The highlighted sperm that acrosome-reacted upon exposure to progesterone don't seem to be moving prior to the addition of progesterone. In contrast, the sperm that spontaneously acrosome react move the whole time. In video 1 this reviewer was not able to identify one sperm that stopped moving upon acrosomal exocytosis. Similarly in video 3, although the resolution of the video makes it difficult to distinguish motile from non-motile sperm. In video 2 the authors only show sperm that are already acrosome reacted. Please explain and provide additional evidence and statistical analysis supporting that sperm stop moving upon acrosomal exocytosis.*

Response R3.5: In videos 1 and 3, the cells are attached to the glass with concanavalin-A, this lectin makes sperm immotile (if well attached) because both the head and tail stick to the glass. The observed motility of sperm in these videos is likely due to them not being properly attached to the glass, which is completely normal. On the contrary, in videos 2 and 4, sperm are attached to the glass with laminin. This is a glycoprotein that only binds the sperm to the glass through its head, that is why they move freely.

*(5) Could the authors provide additional information about the FM4-64 fluorescent dye?*

*What is the mechanism, and how does it visualize structural changes at the flagellum? Since the whole head lights up, does that mean that the dye is internalized and now stains additional membranes, similar to during wound healing assays (PMID 20442251, 33667528). Or is that an imaging artifact? How do the authors explain the correlation between FM4-64 fluorescence increase in the midpiece and the observed change in diameter? Does FM4-64 have solvatochromatic properties?*

Response R3.6: We appreciate the insightful queries posed by Reviewer 3, which echo the concerns initially brought forward by Reviewer 1. For a detailed explanation of the mechanism of FM4-64 dye, how we interpret it, visualizes structural changes in the flagellum,



and its behavior during cellular processes, please refer to our detailed response in Response R1.2. In brief, FM464 is a lipophilic styryl dye that preferentially binds to the outer leaflets of cellular membranes due to its amphiphilic nature. Upon binding, the dye becomes fluorescent, allowing for the visualization of membrane dynamics. The increase in fluorescence in the sperm head or midpiece likely results from the dye's accumulation in areas where membrane restructuring occurs, such as during AE or in response to changes in the flagellum structure.

Regarding the specific questions about internalization and whether FM4-64 stains additional membranes similarly to what is observed in wound healing assays, it's important to note that FM4-64 can indeed be internalized through endocytosis and subsequently label internal vesicular structures. Additionally, FM4-64 may experience changes in its fluorescence as a result of fusion events that increase the lipid content of the plasma membrane, as observed in studies cited (PMID 20442251, 33667528). This characteristic makes FM4-64 valuable not only for outlining cell membranes but also for tracking the dynamics of both internal and external membrane systems, particularly during cellular events that involve significant membrane remodeling, such as wound healing or AE.

Concerning whether the increased fluorescence and observed changes in diameter are artifacts or reflect real biological processes, the correlation observed likely indicates actual changes in the midpiece architecture through molecular mechanisms that remain to be further elucidated. The data presented in Figures 5 and Author response images 6-10 support that this increase in fluorescence is not merely an artifact but a feature of how FM4-64 interacts with its environment.

Finally, regarding the solvatochromatic properties of FM4-64, while the dye does show changes in its fluorescence intensity in different environments, its solvatochromatic properties are generally less pronounced than those of dyes specifically designed to be solvatochromatic. FM464's fluorescence changes are more a result of membrane interaction dynamics and dye concentration than of solvatochromatic shifts.

*(6) For the experiment summarized in Figure S1, did the authors detect sperm that acrosome-reacted upon exposure to progesterone and kept moving? This reviewer is wondering how the authors reliably measure FM4-64 fluorescence if the flagellum moves in and out of the focal plane. If the authors observe sperm that keep moving, what was the percentage within a sperm population and how did FM4-64 fluorescence change?*

Response R3.6: We did identify sperm that underwent acrosome reaction upon exposure to progesterone and continued to exhibit movement. However, due to the issue raised by the reviewer regarding the flagellum going out of focus, we opted to quantify the percentage of sperm that were adhered to the slide (using laminin). This approach allows for the observation of flagellar position over time, facilitating an easy assessment of fluorescence changes. The percentage of sperm that maintained movement after AE is depicted in Figure 1C.

*(7) In Figure S1B it doesn't look like the same sperm is shown in all channels or time points, the hook shown in the EGFP channel is not always pointing in the same direction. If FM4-64 is staining the plasma membrane, how do the authors explain that the flagellum seems to be more narrow in the FM4-64 channel than in the brightfield and DsRed2 channel?*

Response 3.7: It is the same sperm, but due to technical limitations images were sequentially acquired. For example, for time 5 minutes after progesterone, all images in DIC were taken, then all images in the EGFP channel, then DsRed2\* and finally FM4-64. The reason for this

was to acquire images as fast as possible, particularly in DIC images which were then processed to get the beat frequency.

Regarding the flagellum that seems to be more narrow in the FM4-64 channel compared to the BF or DsRed2 channel, the explanation is related to the fact that intensity of the DsRed2 signal is stronger than the other two. This higher signal may have increased the amount of photons captured by the detector.

*(8) Overall, it would be beneficial to include statistics on how many sperm within a population did change FM4-64 fluorescence during AE and how many did not, in addition to information about motility changes and viability. Did the authors exclude that the addition of FM4-64 causes cell death which could result in immotile sperm or that only dying sperm show an increase in FM4-64 fluorescence?*

Response 3.8: The relationship between cell death and the increase in FM4-64 fluorescence is widely discussed in Response P2.3. In our experiments, we always considered sperm that were motile to hypothesize about the relevance of this observation. We have two types of experiments:

(1) Sperm-egg Fusion: In experiments where sperm and eggs were imaged to observe their fusion, sperm were initially moving and after fusion, the midpiece contraction (increase in FM4-64 fluorescence was observed) indicating that the change in the midpiece (that was observed consistently in all fusing cells analyzed), is part of the process.

(2) Sperm that underwent AE: we have observed two behaviours as shown in Figure 1:

a) Sperm that underwent AE and they remain motile without midpiece contraction (they are alive for sure);

b) Sperm that underwent AE and stopped moving with an increase in FM464 fluorescence. We propose that this contraction during AE is not desired because it will impede sperm from moving forward to the fertilization site when they are in the female reproductive tract. In this case, we acknowledge that the cessation of sperm motility may be attributed to cellular death, potentially correlating with the increased FM4-64 signal observed in the midpiece of immotile sperm that have undergone AE. To address this hypothesis, we conducted image-based flow cytometry experiments, which are well-suited for assessing cellular heterogeneity within large populations.

Regarding the relationship between the increase in FM4-64 and AE, we have always observed that AE is followed by an increase in FM4-64 in the head in mice (PMID: 26819478) as well as in human (PMID: 25100708) sperm. This was originally corroborated with the EGFP sperm. However, not all the cells that undergo AE increase the FM4-64 fluorescence in the midpiece.

*(9) The authors report that a fraction of sperm undergoes AE without a change in FM4-64 fluorescence (Figure 1F). How does the  $[Ca^{2+}]_i$  change in those cells? Again statistics on the distribution of a certain pattern within a population in addition to showing individual examples would be very helpful.*

Response 3.9: A recent work shows that an initial increase in  $[Ca^{2+}]_i$  is required to induce changes in flagellar beating necessary for hyperactivation (Sánchez-Cárdenas et al., 2018). However, when  $[Ca^{2+}]_i$  increases beyond a certain threshold, flagellar motility ceases. These conclusions are based on single-cell experiments in murine sperm with different concentrations of the  $Ca^{2+}$  ionophore, A23187. The authors reported that complete loss of motility was observed when using ionophore concentrations higher than 1  $\mu M$ . In contrast, spermatozoa incubated with 0.5  $\mu M$  A23187 remained motile throughout the experiment. Once the  $Ca^{2+}$  ionophore is removed, the sperm would reduce the concentration of this ion to

levels compatible with motility and hyperactivation (Navarrete et al., 2016). However, some of the washed cells did not recover mobility in the recorded time window (Sánchez-Cárdenas et al., 2018). These results would indicate that due to the increase in  $[Ca^{2+}]_i$  induced by the ionophore, irreversible changes occurred in the sperm flagellum that prevented recovery of mobility, even when the ionophore was not present in the recording medium.

Taking into account our results, one possible scenario to explain this irreversible change would be the contraction of the midpiece. Our results demonstrate that the increase in  $[Ca^{2+}]_i$  observed in the midpiece (whether by induction with progesterone, ionomycin or occurring spontaneously) causes the contraction of this section of the flagellum and its subsequent immobilization.

*(10) While the authors results show that changes in  $[Ca^{2+}]_i$  correlate with the observed reduction of the midpiece diameter, they do not provide evidence that the structural changes are triggered by  $Ca^{2+}$  influx. It could just be a coincidence that both events spatially overlap and that they temporarily follow each other. The authors should either provide additional evidence or tone down their conclusion.*

Response 3.10: We agree with the reviewer. As suggested, we have toned down our conclusion.

*(11) Are the authors able to detect the changes in the midpiece diameter independent from FM4-64 or other plasma membrane dyes? An alternative explanation could be that the dyes are internalized due to cell death and instead of staining the plasma membrane they are now staining intracellular membranes, resulting in increased fluorescence and giving the illusion that the midpiece diameter decreased. How do the authors explain that the Bodipy-GM1 Signal directly overlaps with DsRed2 and SIR-actin, shouldn't there be some gap? Since the rest of the manuscript is based on that proposed decrease in midpiece diameter the authors should perform orthogonal experiments to confirm their observation.*

Response 3.11: As requested by the reviewer, we have not used new methods to visualize the change in sperm diameter in the midpiece. In neither of them, a membrane dye was used. First, we have performed immunofluorescence to detect a membrane protein (GLUT3). Second, we have used scanning electron microscopy. The results are now incorporated in the new Figure 2FG. In both experiments, a change in the midpiece diameter was observed. Please, also visit responses P2.5 and Author response images 8 to 10.

Regarding the overlap between the signal of Bodipy GM1 (membrane) and the fluorescence of DsRed2 (mitochondria) and Sir-Actin (F-actin), it is only observed in acrosomereacted sperm, not in acrosome-intact sperm (Figure S4). In our view, these structures become closed after midpiece contraction, and the resolution of the images is insufficient to distinguish them clearly. This issue is also evident in Figure 5B. Therefore, we conducted additional experiments using more powerful super-resolution techniques such as STORM (Figures 5D-F).

*(12) The proposed gap of 200 nm between the actin helix and the plasma membrane, has been observed by TEM? Considering that the diameter of the mouse sperm midpiece is about 1  $\mu$ m, that is a lot of empty space which leaves only about 600 nm for the rest of the flagellum. The axoneme is 300 nm and there needs to be room for the ODFs and the mitochondria. Please explain.*

Response 3.12: Unfortunately, the filament of polymerized actin cannot be observed by TEM. Furthermore, we were discouraged from trying other approaches, such as utilizing phalloidin gold, because for some reason, it does not work properly.

In our view, the 200 nm gap between the actin cytoskeleton and the plasma membrane is occupied by the mitochondria (that is the size that it is frequently reported based on TEM; see <https://doi.org/10.1172/jci.insight.166869>).

*(13) The results provided by the authors do not convince this reviewer that the actin helix moves, either closer to the plasma membrane or toward the mitochondria, the observed differences are minor and not confirmed by statistical analysis.*

Response 3.13: As requested, the title of that section was changed. Moreover, our conclusion is exactly as the reviewer is suggesting: “Since the results of the analysis of SiR-actin slopes were not conclusive, we studied the actin cytoskeleton structure in more detail”. This conclusion is based on the statistical analysis shown in Figure S5D-E.

*(14) The fluorescence intensity of all plasma membrane dyes increases in all cells chosen by the authors for further analysis. Could the increase in SiR-Actin fluorescence be explained by a microscopy artifact instead of actin helix remodeling? Alternatively, can the authors exclude that the observed increase in SiR-Actin might be an artifact caused by the increase in FM4-64 fluorescence? Since the brightness in the head similarly increases to the fluorescence in the flagellum the staining pattern looks suspiciously similar. Did the authors perform single-stain controls?*

Response 3.14: We had similar concerns when we were doing the experiments using SiR-actin. Although we have performed single stain controls to make sure that the actin helix remodelling occurs during the midpiece contraction, we have performed experiments using higher resolution techniques such as STORM using a different probe to stain actin (Phalloidin).

*(15) Should actin cytoskeleton remodeling indeed result in a decrease of actin helix diameter, what do the authors propose is the underlying mechanism? Shouldn't that result in changes in mitochondrial structure or location and be visible by TEM? This reviewer is also wondering why the authors focus so much on the actin helix, while the plasma membrane based on the author's results is moving way more dramatically.*

Response 3.15: This raises an intriguing point. Currently, we lack an understanding of the underlying mechanism driving actin remodeling, and we are eager to conduct further experiments to explore this aspect. For instance, we are investigating the potential role of Cofilin in remodeling the F-actin network. Initial experiments utilizing STORM imaging have revealed the localization of Cofilin in the midpiece region, where the actin helix is situated.

Regarding mitochondria, thus far, we have not uncovered any evidence suggesting that acrosome reaction or fusion with the egg induces a rearrangement of these organelles within the structure. The rationale for investigating polymerized actin in depth stems from the fact that, alongside the axoneme and other flagellar structures such as the outer dense fibers and fibrous sheet, these are the sole cytoskeletal components present in that particular tail region.

*(14) The fact that the authors observe that most sperm passing through the zona pellucida, which requires motility, display high FM4-64 fluorescence, doesn't that contradict the authors' hypothesis that midpiece contraction and motility cessation are connected? Videos confirming sperm motility and information about pattern distribution within the observed sperm population in the perivitelline space should be provided.*

Response 3.14: We believe it is a matter of time, as depicted in Figure 1D, our model shows that first the cells lose the acrosome, present motility and low FM4-64 fluorescence in the midpiece (pattern II) and after that, they lose motility and increase FM4-64 fluorescence in

the midpiece (pattern III). That is why, we think that when sperm pass the zona pellucida they present pattern II and after some time they evolve into pattern III.

*(15) In the experiments summarized in Figure 8, did all sperm stop moving? Considering that 74 % of the observed sperm did not display midpiece contraction upon fusion, again doesn't that contradict the authors' hypothesis that the two events are interdependent? Similarly, in earlier experiments, not all acrosome-reacted sperm display a decrease in midpiece diameter or stop moving, questioning the significance of the event. If some sperm display a decrease in midpiece diameter and some don't, or undergo that change earlier or later, what is the underlying mechanism of regulation? The observed events could similarly be explained by sperm death: Sperm are dying × plasma membrane integrity changes and plasma membrane dyes get internalized ×  $[Ca^{2+}]_i$  simultaneously increases due to cell death × sperm stop moving.*

Response 3.15: The percentage of sperm that did not exhibit midpiece contraction in Fig.8B is 26%, not 74%, indicating that it does not contradict our hypothesis. However, this still represents a significant portion of sperm that remain unchanged in the midpiece, leaving room for various explanations. For instance, it's possible that: i) the change in fluorescence was not detected due to the event occurring after the recording concluded, or ii) in some instances, this alteration simply does not occur. Nevertheless, we did not track subsequent events in the oocyte, such as egg activation, to definitively ascertain the success of fusion. Incorporation of the dye only manifests the initiation of the process.

*(16) The authors propose changes in  $Ca^{2+}$  as one potential mechanism to regulate midpiece contraction, however, the  $Ca^{2+}$  measurements during fusion are flawed, as the authors write in the discussion, by potential  $Ca^{2+}$  fluorophore dilution. Considering that the authors observe high  $Ca^{2+}$  in all sperm prior to fusion, could that be a measuring artifact? Were acrosome-intact sperm imaged with the same settings to confirm that sperm with low and high  $Ca^{2+}$  can be distinguished? Should  $[Ca^{2+}]_i$  changes indeed be involved in the regulation of motility cessation during fusion, could the authors speculate on how  $[Ca^{2+}]_i$  changes can simultaneously be involved in the regulation of sperm hyperactivation?*

Response 3.16: We agree with the reviewer that our experiments using calcium probes are not conclusive for many technical problems. We have toned down our conclusions in the new version of the manuscript.

*(17) 74: AE takes place for most cells in the upper segment of the oviduct, not all of them.*  
*Please correct.*

Response 3.17: Corrected in the new version.

*(18) 88: Achieved through, or achieved by, please correct.*

Response 3.18: Corrected in the new version.

*(19) 243: Acrosomal exocytosis initiation by progesterone, please specify.*

Response 3.19: Modified in the new version.

*(20) 277: "The actin cytoskeleton approaches the plasma membrane during the contraction of the midpiece" is misleading. The author's results show the opposite.*

Response 3.20: As suggested, this statement was modified.

| (21) 298: *Why do the authors find it surprising that the F-actin network was unchanged in acrosome-intact sperm that do not present a change in midpiece diameter?*

Response 3.21: The reviewer is right. The sentence was modified.

| (22) Figures 5D,F: *The provided images do not support a shift in the actin helix diameter.*

Response 3.22: The shift in the actin helix diameter is provided in Figure 5E and 5G.

| (23) Figure S5C: *The authors should show representative histograms of spontaneously-, progesterone induced-, and ionomycin-induced AE. Based on the quantification the SiRactin peaks don't seem to move when the AR is induced by progesterone.*

Response 3.23: As requested, an ionomycin induced sperm is incorporated.

| (24) 392: *Which experimental evidence supports that statement?*

Response 3.24: A reference was incorporated.

Reference 13 is published, please update. Response 3.25: updated as requested.

<https://doi.org/10.7554/eLife.93792.2.sa0>